medRxiv preprint doi: https://doi.org/10.1101/2024.03.18.24304492; this version posted March 19, 2024. The copyright holder for this preprint (which was not certified by peer review) is the author/funder, who has granted medRxiv a license to display the preprint in perpetuity. All rights reserved. No reuse allowed without permission.

Graphene Multiplexed Sensor for Point-of-Need Viral Wastewater-Based Epidemiology

Michael Geiwitz[1], Owen Rivers Page[2], Tio Marello[1], Narendra Kumar[3], Stephen Hummel[4], Vsevolod Belosevich[1], Qiong Ma[1], Tim van Opijnen[2], Bruce Batten[3], Michelle M. Meyer[2], Kenneth S. Burch[1*]

[1] Department of Physics, Boston College, Chestnut Hill, MA 02467, USA

[2] Department of Biology, Boston College, Chestnut Hill, MA 02467, USA

[3] GRIP Molecular Technologies, Inc., 1000 Westgate Drive, Saint Paul, MN 55114, USA

[4] Department of Chemistry and Life Science, United States Military Academy, West Point, NY 10996, USA

Abstract

Wastewater-based epidemiology (WBE) can help mitigate the spread of respiratory infections through the early detection of viruses, pathogens, and other biomarkers in human waste. The need for sample collection, shipping, and testing facilities drives up the cost of WBE and hinders its use for rapid detection and isolation in environments with small populations and in low-resource settings. Given the ubiquitousness and regular outbreaks of respiratory syncytial virus, SARS-CoV-2 and various influenza strains, there is a rising need for a low-cost and easy-to-use biosensing platform to detect these viruses locally before outbreaks can occur and monitor their progression. To this end, we have developed an easy-to-use, cost-effective, multiplexed platform able to detect viral loads in wastewater with several

*Corresponding author at: Department of Physics, Boston College, Chestnut Hill, MA 02467, USA
Email address: ks.burch@bc.edu (K.S. Burch)

NOTE: This preprint reports new research that has not been certified by peer review and should not be used to guide clinical practice.

medRxiv preprint doi: https://doi.org/10.1101/2024.03.18.24304492; this version posted March 19, 2024. The copyright holder for this preprint (which was not certified by peer review) is the author/funder, who has granted medRxiv a license to display the preprint in perpetuity. All rights reserved. No reuse allowed without permission.

orders of magnitude lower limit of detection than mass spectrometry. This is enabled by wafer scale production and aptamers pre-attached with linker molecules, producing forty-four chips at once. Each chip can simultaneously detect four target analytes using twenty transistors segregated into four sets of five for each analyte to allow for immediate statistical analysis. We show our platform's ability to rapidly detect three virus proteins (SARS-CoV-2, RSV, and Influenza A) and a population normalization molecule (caffeine) in wastewater. Going forward, turning these devices into hand-held systems would enable waste-water epidemiology in low-resource settings and be instrumental for rapid, local outbreak prevention.

Keywords

SARS-CoV-2; Influenza; Respiratory syncytial virus; Graphene field effect transistor (GFET); Caffeine; Aptamer

1. Introduction

According to the World Health Organization, lower respiratory infections are the fourth leading cause of death worldwide and second in low-income countries (World Health Organization 2014). The top three causes for these infections are SARS-CoV-2, Influenza, and Respiratory Syncytial Virus (RSV) (Madhi et al. 2020; Rouzé et al. 2021; Lafond et al. 2021). There is a growing emphasis on wastewater-based epidemiology (WBE) to track outbreaks. However, WBE is predominantly performed in high-income countries and densely populated areas (Ahmed et al. 2020; Hart and Halden 2020; Medema et al. 2020). Furthermore, if detection can occur on site, WBE would be instrumental to mitigating and tracking outbreaks from these viruses via early detection of viruses and other pathogens shed by asymptomatic carriers without requiring invasive and frequent individual tests (Champredon and Vanrolleghem 2023). For example, SARS-Cov-2 RNA can be detectable in wastewater 5 – 8 days before

medRxiv preprint doi: https://doi.org/10.1101/2024.03.18.24304492; this version posted March 19, 2024. The copyright holder for this preprint (which was not certified by peer review) is the author/funder, who has granted medRxiv a license to display the preprint in perpetuity. All rights reserved. No reuse allowed without permission.

symptom onset and 2 – 4 days before positive clinical PCR tests (Peccia et al. 2020; Nemudryi et al. 2020).

Indeed, several college campuses exploited existing testing infrastructure to employ highly localized wastewater testing to prevent outbreaks during the Covid-19 pandemic. An instructive example is the University of California San Diego (UCSD), where sampling from 239 buildings across their campus allowed early hot spot detection and individual testing on a per-building basis (Karthikeyan et al. 2021, 2022). UCSD diagnosed nearly 85% of all SARS-CoV-2 infections on campus early and implemented preventative measures to mitigate the spread of the virus (Karthikeyan et al. 2021). This localized approach to WBE could also benefit low- and middle-income countries, where sewage is typically collected in individual or partially shared reservoirs (Street et al. 2020) that are not connected to community sewage systems (Adelodun et al. 2020). This is particularly relevant to RSV, a leading cause of respiratory-related deaths in those 0 – 5 years old (CDC 2023), where data from low- and middle-income countries is lacking or missing altogether due to inadequate systems and infrastructure needed to track disease transmission (Pawar 2023). Even in high-resource settings, the typical collection at a central waste-water facility limits sensitivity of pathogen detection in wastewater due to short half-lives of analytes of interest (Hart and Halden 2020) and natural dilution (Lowry, Wolfe, and Boehm 2023) of target biomarkers.

Several factors have hindered the widespread adoption of WBE and led to the general reliance on sample collection at centralized treatment facilities. Specifically, WBE testing is performed almost entirely utilizing advanced techniques in analytical chemistry and molecular biology, including liquid chromatography-mass spectrometry (LC-MS), high-pressure liquid chromatography-mass spectrometry (HPLC-MS), digital polymerase chain reaction, or real-time quantitative polymerase chain reaction (RT-qPCR) that requires dedicated lab space, personnel, equipment, and chemicals (Lorenzo and Picó 2019). Limited testing facilities and the need for sample collection and transport can also delay results and

medRxiv preprint doi: https://doi.org/10.1101/2024.03.18.24304492; this version posted March 19, 2024. The copyright holder for this preprint (which was not certified by peer review) is the author/funder, who has granted medRxiv a license to display the preprint in perpetuity. All rights reserved. No reuse allowed without permission.

response times, limiting WBE for effective outbreak prevention (Leung 2021). Indeed, the WBE company BioBot in Cambridge, MA, says their average testing time is 11 – 15 days due to the need to test from multiple districts in weekly batches, creating a sample testing backlog (Biobot 2023b). Due to dilution of fecal waste in municipal wastewater, LC-MS and RT-qPCR rely on filtering and concentrating the collected sample (Adams 2020; Li, Wnkui; Zhang, Ji; Tse 2013), with HPLC-MS also subjecting it to several high-pressure steps to separate constituent elements (Else et al. 2010; Metabolite et al. 2023). Thus, a low-cost, easy-to-use, multiplexed device is urgently needed to enable point-of-need WBE.

Particularly challenging is the need of a sensing platform to withstand the harsh wastewater medium while accurately and reliably distinguishing between the various components. Wastewater can contain viruses shed in human waste and other particles ranging from naturally occurring biomass, bacteria strains, and drug metabolites to pharmaceuticals (Massano et al. 2023). Similarly challenging is the need to multiplex assays or testing strategies to monitor multiple targets to reduce cost, time, and effort while addressing seasonal and population variations via normalization. For point-of-need WBE sensing, population normalization is crucial due to increased variability in dilution factors, such as per capita water use, stormwater inputs, etc., and viral shedding rates (Sweetapple et al. 2023; Rainey et al. 2023; C. Li et al. 2022a). This variability exacerbates the already challenging task of calculating the number of people infected based solely on the virus concentration in the wastewater sample. For example, depending on the level of infection, a person suffering from SARS-CoV-2 can excrete anywhere from 600,000 (N. Zhang et al. 2020) to 30,000,000 virions/L (Wölfel et al. 2020) of fecal matter.

To enable WBE at the local level, especially in low-resource and rural communities, it is helpful to look towards efforts in personalized health care. Substantial efforts have been made regarding sensing respiratory infections using lateral flow immunoassay (LFIA), low-cost PCR, and electronic sensors. Electronic sensors are potentially the most promising as they can simultaneously offer multiplexed, low-cost, high sensitivity detection with minimal human effort. Here, there is growing

medRxiv preprint doi: https://doi.org/10.1101/2024.03.18.24304492; this version posted March 19, 2024. The copyright holder for this preprint (which was not certified by peer review) is the author/funder, who has granted medRxiv a license to display the preprint in perpetuity. All rights reserved. No reuse allowed without permission.

interest in graphene field effect transistors (GFET), which have shown the capability to detect everything from lead ions (Velusamy et al. 2022; Dong et al. 2023) to bacteria and oral disease biomarkers (Ping et al. 2016b; Gao et al. 2016; Kumar, Gray, et al. 2020), though few have shown multiplexing capabilities (Lu et al. 2022; Kumar et al. 2022; Kumar, Gray, et al. 2020). Nonetheless, only two groups, including ours, have demonstrated GFET's use for detection of analytes in wastewater. For instance, a GFET recently detected cadmium ions in wastewater with a limit of detection (LOD) of 0.125 pM (H. Wang et al. 2023). Still, virus protein detection in wastewater with GFETs, let alone by a scalable fabrication method, has not been shown.

This work focused on developing wafer-scale fabrication of GFET devices for rapid, easy-to-use, low-cost, multiplexed, and population-normalized detection of respiratory viruses in wastewater at low levels of detection (LOD). To do so, we implemented a new probe strategy where aptamers, single-stranded oligonucleotides, are pre-attached to the linker molecule, removing the need for harsh solvents. This enhanced the device's reproducibility, lowering filtration levels and producing better LOD. In addition, we have optimized the fabrication process to make 44 chips simultaneously on a four-inch wafer. The devices are tested using freshly collected waste-water samples to detect SARS-CoV-2 spike protein, Influenza A hemagglutinin, RSV glycoprotein, and caffeine for comparison with lab-based WBE methods.

2. Materials and Methods

2.1 Graphene Platform Development

2.1.1 Graphene as a transducer

Graphene is particularly useful yet challenging as a transducer due to its extreme sensitivity to surface charges (Castro Neto et al. 2009; Ping et al. 2016a; Hwang et al. 2016). Nonetheless, graphene is biocompatible and can be prepared at wafer scale. Due to its zero-band gap, it has a well-defined Dirac

medRxiv preprint doi: https://doi.org/10.1101/2024.03.18.24304492; this version posted March 19, 2024. The copyright holder for this preprint (which was not certified by peer review) is the author/funder, who has granted medRxiv a license to display the preprint in perpetuity. All rights reserved. No reuse allowed without permission.

point (charge neutrality point) where its valence and conduction bands meet. This produces a peak in resistance when the chemical potential reaches the Dirac point (Fig. 1). When biomolecules attach to the surface of the graphene, it is generally assumed charge is transferred to graphene either directly or from conformal changes in the probe (J. Li et al. 2021; Seo et al. 2020a). This enables quantification of the target concentration via a shift in voltage at which the Dirac point appears.

Another advantage of graphene is the ease of functionalization with the biomolecules used as probes (Pinto, Gonçalves, and Magalhães 2013). These probes can be bonded to aromatic rings (e.g., Pyrene), which attach to the graphene through π-π stacking. This allows for tremendous biocompatibility between graphene and a host of biomolecules without unintentional disorder from chemical bonding. However, typically, graphene is functionalized via a two-step process, where the linker molecule is attached using dimethylformamide (DMF), and then the probe is later bound to the linker molecule (Seo et al. 2020b; Kwong Hong Tsang et al. 2019; https et al. 2022; Nekrasov et al. 2022). Unfortunately, the DMF tends to react with the device, causing instability, higher LOD, and lower reproducibility, and can attack polymers and passivation layers, degrading the device (Khan and Song 2021). As described later, we have avoided this issue and improved the LOD and reproducibility needed for point-of-need WBE using probes pre-attached to the linker molecule and incubated in PBS.

Likewise crucial for detection in complex wastewater matrices, graphene is insensitive to the sample medium's pH levels (Fu et al. 2011). We demonstrated this in our recent work on opioid metabolite detection in wastewater (Kumar et al. 2022), in which we showed the simultaneous detection of Noroxycodone, Norfentanyl, and EDDP (2-ethylidene-1, 5-dimethyl-3, 3-diphenylpyrrolidine) with an LOD below that of HPLC-MS (Kumar et al. 2022). This work also exhibited our platform’s robustness and selectivity of the target molecules in wastewater. Unlike traditional field-effect transistor (FET) sensors that require large gate voltages (>60V) (Ping et al. 2016a), we have

medRxiv preprint doi: https://doi.org/10.1101/2024.03.18.24304492; this version posted March 19, 2024. The copyright holder for this preprint (which was not certified by peer review) is the author/funder, who has granted medRxiv a license to display the preprint in perpetuity. All rights reserved. No reuse allowed without permission.

demonstrated our ionic liquid-gated GFETs are compatible with simple electronics requiring less than 2V (Kumar, Gray, et al. 2020; Kumar, Wang, et al. 2020).

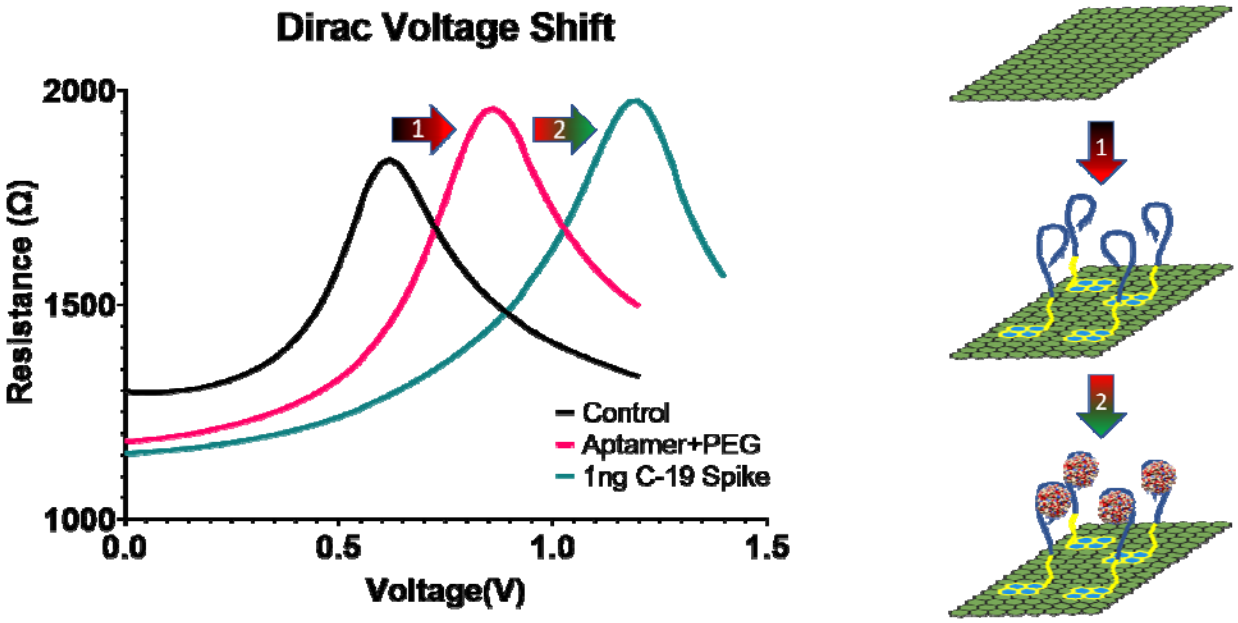

Fig. 1 – Dirac voltage shifting with aptamer and target attachment: The plot on the left shows the positive shift in the Dirac point (peak of the curves) from the intrinsic position of the bare graphene (black) of approximately 0.6V. After a 2:1 mixture of the aptamer probe to PEG is added the Dirac point shifts positively to about 0.8V (pink). A large shift in the Dirac point to 1.2V is then seen (green) in the presence of 1ng/ml of the target protein for SARS-CoV-2. On the right is a schematic of the bare graphene, aptamer attachment, and target attachment.

2.1.2 GFET Fabrication, Characterization, and Functionalization

To bring our GFET-based Graphene Electronic Multiplexed Sensor (GEMS) towards point-of-need WBE, we modified our fabrication method and device design to enable production on a four-inch silicon wafer (Fig. 2a – Top) before dicing into individual chips. This has drastically reduced our costs per chip primarily due to a drastic decrease in fabrication time. Prior to wafer-scale fabrication, we were able to produce 6 – 8 chips in four days. We can now produce 44 GEMS in the same amount of time. Each GEMS has 20 GFETs arranged in groups of five for rapid statistical analysis of variability between GFET devices. To enable multiplexed detection, the groups are segregated with PDMS wells with individual coplanar side gates (Fig. 2b). This enables individual functionalization of each well with a different probe without cross-functionalization.

medRxiv preprint doi: https://doi.org/10.1101/2024.03.18.24304492; this version posted March 19, 2024. The copyright holder for this preprint (which was not certified by peer review) is the author/funder, who has granted medRxiv a license to display the preprint in perpetuity. All rights reserved. No reuse allowed without permission.

We first pattern bottom contacts on a four-inch Si/SiO_2 wafer using bi-layer photoresist (LOR1A/S1805) and photolithography followed by e-beam deposition of 5 nm of titanium wetting layer and 20 nm of platinum. Platinum is chosen to minimize contact resistance to graphene because it is robust and has low surface potential (Fujii, Kasuya, and Kurihara 2017). After metal liftoff, the contacts were annealed under vacuum for 10 hours at 400°C to remove any remaining photoresist and increase the electrodes' smoothness, allowing for better graphene attachment. CVD graphene was transferred on top of the entire wafer by General Graphene Corp. in Knoxville, TN. The wafer was then annealed under vacuum in the e-beam chamber for nine hours at 300°C to remove any remaining residues and water from the transfer process. Before removing from the e-beam chamber, 3 nm of aluminum oxide (AlOx) was deposited to protect the graphene from further chemicals and atmosphere during later fabrication steps. Once removed, the wafer was baked on a hotplate in our glovebox at 175°C for five minutes to ensure aluminum oxide adhesion. The same bi-layer resist process and photolithography system were then used to pattern the graphene for etching via oxygen plasma. The MF-321 developer (from Kayaku) used to develop the pattern after lithography has the added benefit of also removing the 3 nm of AlOx from atop the graphene we wish to etch. This was followed by argon plasma to remove any oxide layer formed on the platinum by the oxygen plasma on the coplanar side gate. Failing to remove this layer has led to higher initial Dirac points and, in turn, lower sensitivity in our devices.

Next, the devices were cleaned with Remover PG and rinsed with IPA and DI water. The chips were then baked under a vacuum at 200°C for one hour to remove any water and clean any residue from the wafer. After this, a 50 nm passivation layer of aluminum oxide was deposited to encapsulate the devices while the wafer was still hot. Oxygen was flowed to achieve a pressure of ~10^5 Torr during AlOx deposition to replenish oxygen stripped from the AlOx crystals during e-beam deposition. A final single layer (S1805) photolithography step was then performed to expose the graphene sensing windows (10um x 40um) and the contact pads for wire bonding. Exposed AlOx was then etched with

medRxiv preprint doi: https://doi.org/10.1101/2024.03.18.24304492; this version posted March 19, 2024. The copyright holder for this preprint (which was not certified by peer review) is the author/funder, who has granted medRxiv a license to display the preprint in perpetuity. All rights reserved. No reuse allowed without permission.

65:35 diluted TRANSETCH-N (from Transene) for 14 minutes at 80°C, then rinsed with DI water. The remaining photoresist was then removed with Remover PG and rinsed with IPA and DI water. The wafer was then diced using a Pelco Wafer Dicing system, eliminating the need for a wafer dicing saw and its associated chemicals. The chips were then mounted to chip carriers and wire-bonded. Following this, PDMS wells made in-house with custom 3D-printed molds were placed on the chips to hold the

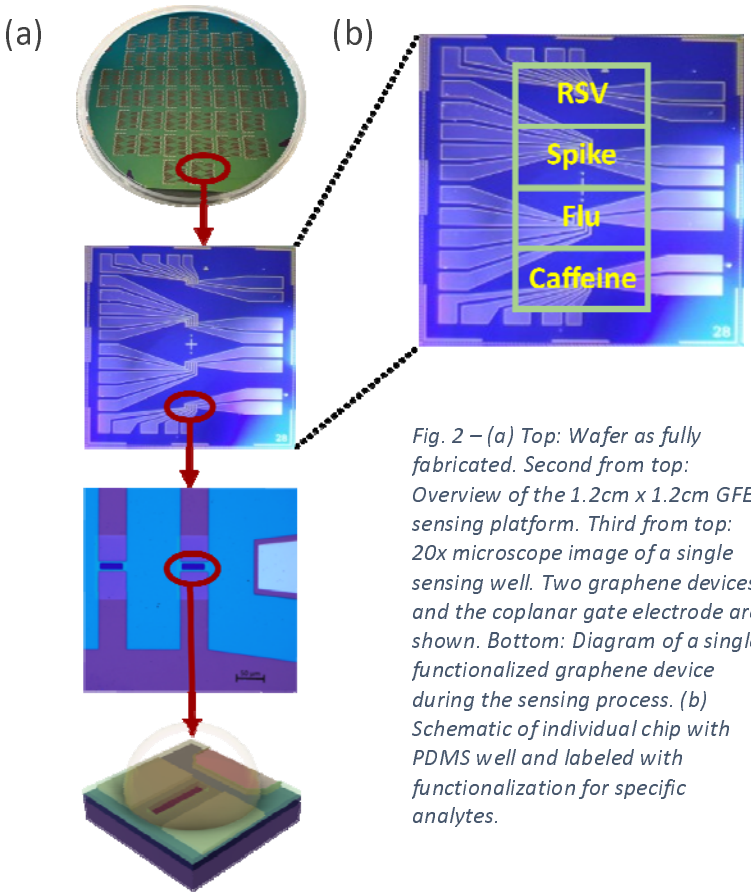

Fig. 2 – (a) Top: Wafer as fully fabricated. Second from top: Overview of the 1.2cm x 1.2cm GFET sensing platform. Third from top: 20x microscope image of a single sensing well. Two graphene devices and the coplanar gate electrode are shown. Bottom: Diagram of a single, functionalized graphene device during the sensing process. (b) Schematic of individual chip with PDMS well and labeled with functionalization for specific analytes.

functionalization liquids and target mixtures during incubation as per our sensing protocols.

2.2 Pre-Linked Aptamers

We employ aptamer probes due to their high affinity, stability, and small size (Cai et al. 2018; Urmann et al. 2017). Aptamer-based protein biosensing depends on aptamer-target binding (Y. Wu et al. 2014), which several factors can complicate. Structurally complex protein targets have more binding sites and interaction types than small molecules (S. Jones et al. 2001; Kohlberger and Gadermaier 2022).

medRxiv preprint doi: https://doi.org/10.1101/2024.03.18.24304492; this version posted March 19, 2024. The copyright holder for this preprint (which was not certified by peer review) is the author/funder, who has granted medRxiv a license to display the preprint in perpetuity. All rights reserved. No reuse allowed without permission.

This increase in complexity can result in aptamers with decreased target specificity if the experimental design of SELEX is flawed (Qian et al. 2022). Generation of aptamers for proteins via SELEX is more manageable for small molecules (Y. Wu et al. 2014), but the conformation of the protein (purified or native) can alter or hinder aptamer binding (Zhou and Rossi 2017; Z. Zhang et al. 2021). Careful consideration is necessary to ensure binding conditions mirror real-world binding conditions. With this in mind, we chose the Universal Aptamer (UA) (Bhardwaj et al. 2019; Shiratori et al. 2014; C.-H. Wang, Chang, and Lee 2016) for Influenza A hemagglutinin, H8 (Percze et al. 2017) for RSV, and 1C (Y. Zhang, Juhas, and Kwok 2022) for SARS-CoV-2 spike proteins based on their binding affinities to their targets. See the Supplemental for further information regarding the aptamers.

Generally, to attach the aptamer to graphene, the device is first incubated with 10 mM 1-pyrenebutyric acid N-hydroxysuccinimide ester (PBASE) linker molecule dissolved in DMF for one hour. After performing a Dirac point measurement to see the shift due to DMF and PBASE, a 2:1 mixture of aptamer to polyethylene glycol (PEG) is incubated for one hour. Adding PEG to the probe mixture has been widely employed (Szunerits et al. 2023; Rodrigues et al. 2022) to prevent unwanted attachment of molecules to any unlinked PBASE molecules and provide space between aptamers, limiting their interactions. The PEG also stabilizes the devices by minimizing drift and standard deviation between different devices.

To further reduce cost, analysis, and fabrication time and boost reproducibility, we altered this typical process by pre-attaching the aptamers and PEG to the PBASE molecules (See supplementary information for more details regarding pre-linking.). Indeed, DMF is known to dope graphene (G. Wu et al. 2017) and thus would be expected to result in a higher limit of detection. With this in mind, we performed identical experiments with GEMS using the standard DMF attachment procedure and our pre-linked PEG (PL-PEG) and probes (PL-aptamers). As seen in Fig. 3 and Table 1, more significant Dirac point shifts occurring at much lower LODs are seen in devices with pre-linked (PL) probes. Lastly, to

medRxiv preprint doi: https://doi.org/10.1101/2024.03.18.24304492; this version posted March 19, 2024. The copyright holder for this preprint (which was not certified by peer review) is the author/funder, who has granted medRxiv a license to display the preprint in perpetuity. All rights reserved. No reuse allowed without permission.

ensure graphene cleanliness and device reproducibility, much of the fabrication was carried out in a pure argon environment inside our cleanroom-in-a-glovebox (Gray et al. 2020).

2.3 Optimization in PBS

2.3.1 Viral aptamers

Selectivity and concentration analysis was first conducted in 1x PBS to determine the aptamer viability without the background signal from wastewater. Specifically, the numerous constituent components in wastewater (Henze, Mogens; van Loosdrecht, Mark; Ekama, George; Brdjanovic 2008; M. H. Huang, Li, and Gu 2010; Novo et al. 2013), many of which are charged ions, can produce false positives. For each target, we first determined the initial Dirac point of the graphene in 0.01x PBS (see Supplemental). Diluted PBS minimizes the Debye screening effect (Stern 2007). Typically, we observe a Dirac point around 0.6 V ($\pm$0.1V) due to the work function of the platinum side gate electrode (Fujii, Kasuya, and Kurihara 2017). This baseline Dirac point ensures the graphene quality without unwanted doping. This is further confirmed by the nearly symmetric slopes to the left (hole regime) and to the right (electron regime) of the Dirac point, which results from the charge carrier mobilities (Gosling et al. 2021). Passivation issues are typically indicated by double peaks in the curves. Good passivation is also confirmed by ensuring the Dirac point does not drift with repeated gate voltage sweeps. The highest quality devices have an initial Dirac point in the range of 0.58 – 0.7 V with an average starting resistance around 2000 Ω and a stable Dirac point after three measurements. Data on initial Dirac point and starting resistances were collected for 545 different GFETs fabricated over two years in our lab, showing that most of our devices fall within these parameters (see Supplemental).

After initial testing, we incubated the graphene devices for one hour with a 2:1 mixture of 10uM PL-aptamer to 10uM PL-PEG, which was optimized in our previous work with opioids in wastewater and oral disease biomarkers in saliva (Kumar, Wang, et al. 2020; Kumar, Gray, et al. 2020; Kumar et al. 2022).

medRxiv preprint doi: https://doi.org/10.1101/2024.03.18.24304492; this version posted March 19, 2024. The copyright holder for this preprint (which was not certified by peer review) is the author/funder, who has granted medRxiv a license to display the preprint in perpetuity. All rights reserved. No reuse allowed without permission.

Dirac point measurements are again conducted in 0.01x PBS to confirm attachment to the graphene surface. Upon attachment, the charged phosphate backbone of the aptamer induces positive charge carriers into the graphene, producing a positive 150-200mV shift in the Dirac point (see Supplemental). Atomic force microscopy and Raman measurements have also been performed to confirm the attachment (see Supplemental).

We first assessed all aptamer selectivity against a negative control. For example, the Influenza A hemagglutinin (HA) with a concentration of 10 – 100 ng/ml that is far beyond that found in wastewater (tens of pg/ml), is incubated on the devices for one hour in the well containing the SARS-COV-2 SPIKE PROTEIN aptamer (1C). No shift in the Dirac point was seen, showing the HA protein does not bind to the 1C aptamer (Fig. 3 – Covid). Similar negative control analyses were conducted in the wells functionalized with the Influenza and RSV aptamers. As shown in Fig. 3, these aptamers had a slightly higher non-specific interaction with the negative control proteins. Nonetheless, the Dirac point shifts in wells with the Influenza and RSV aptamers resulting from negative controls were relatively small (approximately 50 mV), setting the baseline for future measurements.

Next, we focused on assessing each aptamer's limit of detection and affinity. We followed a standard protocol of incubating the devices with a specific concentration of the target proteins. After incubation, the device is rinsed with 1x PBS and DI water before performing the Dirac point measurement in 0.01x PBS. For each concentration, the reported shift is the difference in the Dirac point value obtained from that of the negative control. After measuring the Dirac shift, we incubated with increasing target protein concentrations. To ensure the absence of systematic errors, we have also performed measurements with random concentrations to ensure they match the signal detected by a systematic increase in concentration.

medRxiv preprint doi: https://doi.org/10.1101/2024.03.18.24304492; this version posted March 19, 2024. The copyright holder for this preprint (which was not certified by peer review) is the author/funder, who has granted medRxiv a license to display the preprint in perpetuity. All rights reserved. No reuse allowed without permission.

Beginning with low concentration, each incubation is conducted for one hour. We found that concentrations below 1 fg/ml for the SARS-COV-2 spike protein did not change the Dirac point. However, the RSV and HA proteins produced shifts at much lower concentrations (approximately 10 ag/ml). This shift discrepancy may be due to the newness of the SARS-COV-2 spike aptamer and future improvements can improve its binding affinity. The average shift from all devices in the well and their standard deviations are plotted in the same graph as the negative control's shift. The concentrations are increased by one order of magnitude in each subsequent incubation, and the same rinsing and sensing

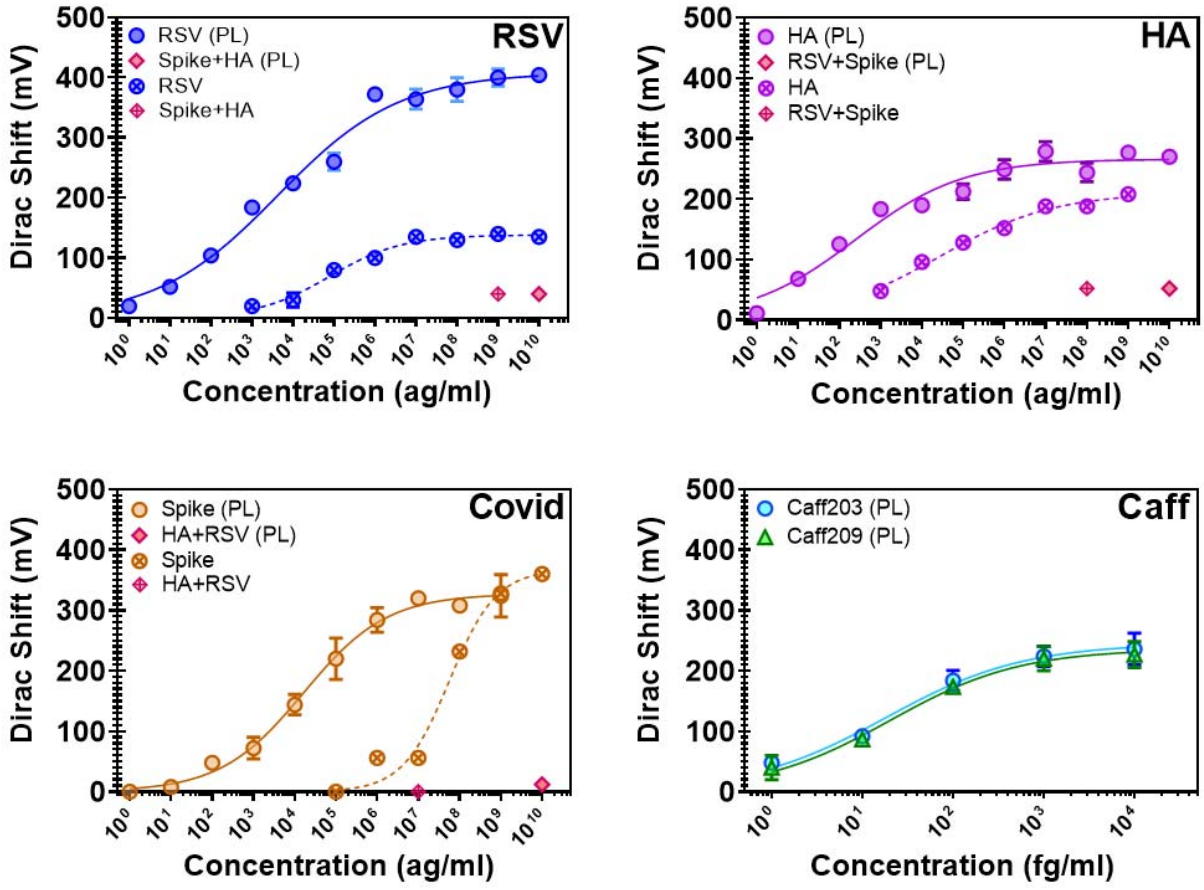

Fig. 3 –Concentration dependance measurements of viral proteins in PBS. Error bars calculated from the five GFETs per sensing well. Data points with crosses and dashed curves indicate non-pre-linked aptamers were used. Top Left - Influenza A Hemagglutinin detection. High concentrations of RSV and COVID Spike proteins used as a negative control. (PL) denotes pre-linked aptamer experiment. Top Right and Bottom Left - Same as in HA plot but with SARS-CoV-2 Spike and RSV proteins, respectively. Non-target proteins used as negative control in each case. Bottom Right - Concentration dependence measurements of two caffeine aptamers. Caffeine measurements were only conducted with pre-linked aptamers.

medRxiv preprint doi: https://doi.org/10.1101/2024.03.18.24304492; this version posted March 19, 2024. The copyright holder for this preprint (which was not certified by peer review) is the author/funder, who has granted medRxiv a license to display the preprint in perpetuity. All rights reserved. No reuse allowed without permission.

protocol is conducted for each. The concentrations are increased until a saturation point is reached, determined by no further shift with two consecutive high concentrations.

Upon collecting the concentration dependence, we found the binding characteristics of the aptamer by fitting the Dirac voltage shift versus target analyte concentration to Hill's equation (Goutelle et al. 2008):

$$V_D = \frac{V_D^{max} * C^n}{K_D^n + C^n} \quad (1)$$

Here, V_D is the Dirac voltage shift measured in mV, V_D^{max} is the maximum Dirac voltage shift at the saturation point, C is the concentration of the target analyte, n is the Hill Coefficient determined to be the maximum slope on a log plot of the response curve, and K_D is the dissociation constant. The parameters were found using a least squares fit model in Matlab after providing estimates of the Hill Coefficient, maximum Dirac voltage, and dissociation constant. Due to the five devices in each well of the GFET, we can perform statistical analysis immediately. This allows us to calculate the LOD for each analyte by using the residuals of the standard deviation against the Hill fit using 3σ analysis (Belter, Sajnóg, and Barałkiewicz 2014):

$$LOD = \frac{3\sigma}{n} \quad (2)$$

Here, σ is the standard deviation from the fit and n is again the Hill slope. This was used to find the LODs in Table 1.

medRxiv preprint doi: https://doi.org/10.1101/2024.03.18.24304492; this version posted March 19, 2024. The copyright holder for this preprint (which was not certified by peer review) is the author/funder, who has granted medRxiv a license to display the preprint in perpetuity. All rights reserved. No reuse allowed without permission.

Table 1 *Comparison of LODs between pre-linked and unlinked aptamers for each target analyte in PBS. All pre-linked virus experiments were conducted on a single GFET chip and unlinked on another. Caffeine experiments were only performed with pre-linked aptamers and done on a single GFET chip.*

Target	Unlinked Aptamer	Pre-Linked Aptamer
SARS-CoV-2 Spike Protein	91 pg/ml	55 ag/ml
Hemagglutinin (Flu A)	79 fg/ml	408 ag/ml
Respiratory Syncytial Virus Protein	43 fg/ml	453 ag/ml
Caffeine	N/A	Caff203: 35 fg/ml Caff209: 26 fg/ml

2.3.2 Caffeine aptamer

WBE programs use several different biomarkers to determine the total contributing population. These include caffeine, paraxanthine (caffeine's metabolite), creatine, 5-hydroxyindoleacetic acid (5-HIAA, serotonin metabolite), and pepper mild mottle virus (PMMoV) given their ubiquitousness in human diets and survivability in wastewater (Hsu et al. 2022). Paraxanthine and PMMoV concentration, in particular, are excellent means for population normalization (C. Li et al. 2022b). Unfortunately, to the best of our knowledge, no aptamer has yet been developed for PMMoV or paraxanthine. Therefore, to test our platform's capabilities as a means for population normalization in wastewater, two previously reported caffeine aptamers were selected based on their reported results that show micromolar sensitivity in human serum (P. J. J. Huang and Liu 2022), two of which (Caff203 and Caff209) were chosen for our tests in wastewater. Both the Caff203 and Caff209 aptamers were pre-attached to the PBASE linker molecules, and the same functionalization and sensing protocols were followed as the virus proteins. Both were evaluated first in PBS to determine their viability before exposure to wastewater. Caff203 was found to have an LOD of 35 fg/ml in PBS, while Caff209 showed 26 fg/ml in PBS (Fig. 3). Due to its lower LOD, Caff209 was selected for future experiments.

medRxiv preprint doi: https://doi.org/10.1101/2024.03.18.24304492; this version posted March 19, 2024. The copyright holder for this preprint (which was not certified by peer review) is the author/funder, who has granted medRxiv a license to display the preprint in perpetuity. All rights reserved. No reuse allowed without permission.

3. Results

3.1 Wastewater biosensing

3.1.1 Wastewater dilution optimization

Next, we turned to testing GEMS with wastewater. In our earlier work on opioid metabolites, we found diluting the wastewater with 1x PBS to a 20:1 mixture necessary to minimize unwanted Dirac point shifts and false positives from the myriad components and non-neutral pH (6-9). Given the improved device performance with pre-attachment, we re-optimized this dilution to attempt a lower LOD. We began by incubating the 1C PL-aptamer and PL-PEG, as previously discussed. The wastewater was then passed through a 0.3-micron filter to remove large particulates. Next, various dilutions (2:1, 5:1, 10:1, and 20:1) were incubated directly on the devices for one hour, and the resulting Dirac point shift is shown in Fig. 4. We found the 10x dilution caused an approximate 60 mV Dirac point shift, the same as the 20x dilution. Since PBS does not induce a shift, the background signal from wastewater will increase the LOD by setting a floor below which we cannot uniquely detect the target, as indicated by the horizontal dashed lines in Fig. 5. Next, four samples were diluted with the 2:1, 5:1, 10:1, and 20:1

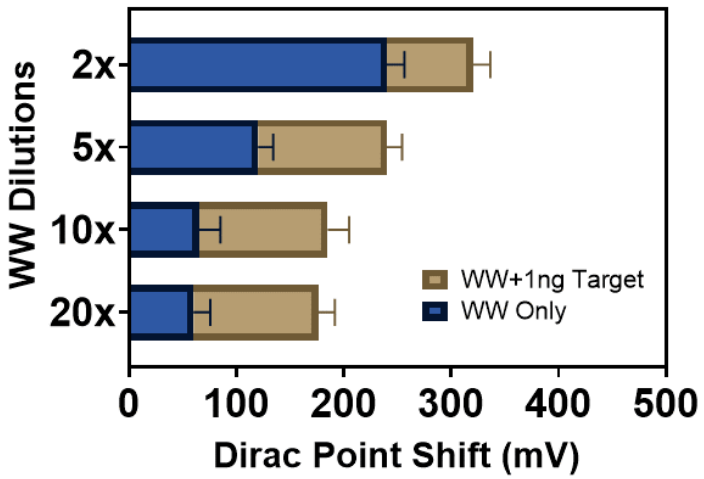

Fig. 4 – Histogram of the average Dirac point shift at various wastewater dilutions. The blue areas show the average Dirac point shift for five GFET devices after incubation of diluted wastewater for one hour. The tan areas show the further Dirac point shift after incubating the GFETs for one hour with 1ng/ml of target protein in their respective wastewater dilutions.

medRxiv preprint doi: https://doi.org/10.1101/2024.03.18.24304492; this version posted March 19, 2024. The copyright holder for this preprint (which was not certified by peer review) is the author/funder, who has granted medRxiv a license to display the preprint in perpetuity. All rights reserved. No reuse allowed without permission.

PBS to wastewater samples to create 1 ng/ml solutions of SARS-COV-2 spike protein and incubated on the devices for one hour. This was done to determine if wastewater dilution affected the ability of the aptamers to find the target proteins. The 1 ng/ml concentration was used since this is the point at which the SARS-COV-2 SPIKE PROTEIN aptamer saturated when tested in 1x PBS. Interestingly, there was a statistically insignificant difference in the shift between the 10:1 and 20:1 wells. Both measured a shift of around 130 mV after incubating with the spike protein mixture. Thus, we focused 10:1 PBS to wastewater dilution to achieve the smallest possible LOD in wastewater.

3.1.2 Detection of Analytes in Wastewater

Having optimized the wastewater dilution, we performed a similar series of concentration-dependent measurements with the same protocol done first in PBS. The experiments were conducted in two rounds for each analyte. Experiments were first performed on a single GFET chip. Four wells were functionalized with a different pre-attached aptamer: 1C for SARS-CoV-2, UA for hemagglutinin, H8 for RSV, and Caff209 for caffeine. A fresh wastewater sample was obtained (collected one day prior and stored a 4°C overnight), filtered, and diluted in a 10:1 ratio with PBS and spiked with virus proteins and caffeine to make concentrations ranging from 1 fg/ml to 1 ng/ml with an increase of one order of magnitude between each concentration. The second round of experiments was conducted one month later using a newly fabricated GFET chip, fresh pre-attached aptamers, and a new wastewater sample. In both instances, the negative controls were tested first at 1 ng/ml to check selectivity, followed by increasing the concentrations of the target analyte. In both rounds, the negative controls showed little to no shift beyond the background 60mV shift from the wastewater (dashed lines in Fig. 5).

The resulting concentration curves are shown in Fig. 5, and LODs for each round are shown in Table 2. As expected, LOD values increased over the PBS results due to the intrinsic 60mV signal from the wastewater. Nonetheless, the larger LODs are all well within the range for the concentrations of

medRxiv preprint doi: https://doi.org/10.1101/2024.03.18.24304492; this version posted March 19, 2024. The copyright holder for this preprint (which was not certified by peer review) is the author/funder, who has granted medRxiv a license to display the preprint in perpetuity. All rights reserved. No reuse allowed without permission.

each analyte in wastewater. SARS-CoV-2 has been shown to contain 24±9 spike proteins per virion (Ke et al. 2020), theoretically suggesting the LOD for our GEMS platform to be on the order of 27 – 59 virions/ml (27,000 – 59,000 virions/L) in wastewater assuming fully lysed virions. Influenza A has been found to contain 300 – 400 HA proteins per virion (Einav, Gentles, and Bloom 2020), giving a theoretical LOD of fully lysed virions in the 1.5 – 7 virions/ml (1,500 – 7000 virions/L). To the best of our knowledge, the average number of proteins for RSV has not yet been determined. Assuming a similar number between the spike and the Influenza A proteins, the theoretical, fully lysed RSV virions could be 15 – 397 virions/ml (15,000 – 397,000 virions/L). Like the experiments conducted in PBS, the RSV and SARS-COV-2 spike aptamers show little to no shift with the high concentration of negative control. In contrast, the HA aptamer showed a small but significant shift of around 60 mV with negative control. This could be partly due to UA's longer length compared to the others, allowing it to bind to more constituent elements in the wastewater. It could also be due to HA proteins already present in the wastewater sample, which was collected during the 2022 – 2023 Flu season.

Due to its lower LOD found in PBS (Table 1), Caff209 was selected for analysis in wastewater. Interestingly, the LOD in wastewater was lower than in PBS, which was not seen with the virus proteins. This could be due in part to the salt content in wastewater facilitating binding (Lores and Pennock 1998) of the much smaller caffeine molecules, which are 0.194 kDa as compared to the larger proteins having sizes of 139.7 kDa, 59 kDa, and 37 kDa for spike, HA, and RSV respectively, lowering the variability between the devices.

medRxiv preprint doi: https://doi.org/10.1101/2024.03.18.24304492; this version posted March 19, 2024. The copyright holder for this preprint (which was not certified by peer review) is the author/funder, who has granted medRxiv a license to display the preprint in perpetuity. All rights reserved. No reuse allowed without permission.

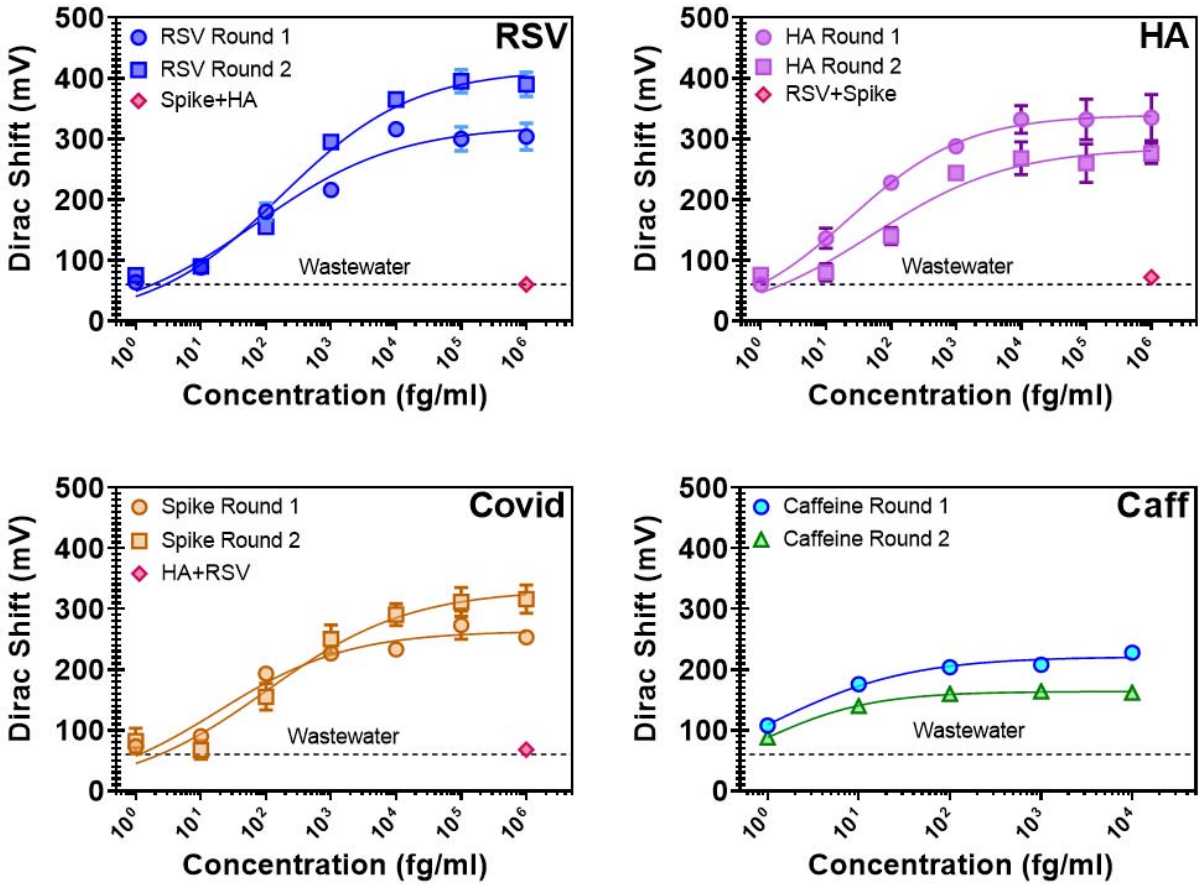

Fig. 5 – Concentration dependence measurements of viral proteins and caffeine in wastewater. Error bars calculated from the five GFETs per sensing well. From left to right, HA, RSV, and COVID spike proteins and Caffeine. Horizontal dashed line shows intrinsic background shift from the wastewater itself.

345 To put these LODs in context, we compare them with other reported LODs. BioBot reports a
346 limit of detection (LOD) for SARS-CoV-2 of 9000 copies/L using RT-qPCR (Biobot 2023a) (approximately
347 10 whole virions/L), which is lower than concentrations typically found in wastewater. The reliance on
348 lab testing results from these low virus loads in wastewater requires amplification and/or viral
349 concentration steps to detect. These concentrations can range from, in the case of SARS-CoV-2, 150,000
350 – 141.5 million viral genome copies (150 – 141,500 whole virions (Sender et al. 2020)) per liter of
351 wastewater (Hart and Halden 2020). Influenza A concentrations are reported to be around 260,000
352 copies per liter (Heijnen and Medema 2011) and RSV 1,071 – 70,700 copies per liter (Ahmed et al. 2023).
353 Others have reported LODs from RT-qPCR as low as 2.9 – 4.6 copies per reaction after concentrating the

medRxiv preprint doi: https://doi.org/10.1101/2024.03.18.24304492; this version posted March 19, 2024. The copyright holder for this preprint (which was not certified by peer review) is the author/funder, who has granted medRxiv a license to display the preprint in perpetuity. All rights reserved. No reuse allowed without permission.

354 sample from 50ml to 20ul (Ahmed et al. 2022). Several studies have found levels of shed virus can vary
355 substantially depending on patient infection level and virus variants, ranging from $10^2 – 10^7$ copies/ml
356 (D. L. Jones et al. 2020; Pan et al. 2020; Zang et al. 2020; Han et al. 2020). These levels will significantly
357 decrease upon reaching a wastewater treatment facility due to dilution and virus decay, highlighting the
358 need for more localized collection and analysis. While our GEMS platform cannot achieve the low LODs
359 seen with RT-qPCR, its LODs are 1 – 2 orders of magnitude lower than what has been reported with LC-
360 MS (Table 2).

Table 2
Limits of Detection (LOD) for each target analyte from two separate experimental rounds. Each round was conducted on a single GFET chip. Based on their average molecular weights, LODs were converted from fg/ml to proteins/ml.

Target	Round 1 LOD	Round 2 LOD	Reported LC-MS from Literature
SARS-CoV-2 Spike Protein	136 fg/ml (890 proteins/ml)	187 fg/ml (1224 proteins/ml)	$10^5 – 10^6$ copies/ml (Griffin and Downard 2021; Dollman, Griffin, and Downard 2020; Nikolaev et al. 2020; Picó and Barceló 2021) (~3000 fg/ml)
Hemagglutinin (Flu A)	39.6 fg/ml (612 proteins/ml)	181 fg/ml (2799 proteins/ml)	$7x10^6$ copies/ml (Bojórquez-Velázquez et al. 2022) (~30,000 fg/ml)
Respiratory Syncytial Virus glycoprotein	176 fg/ml (5927 proteins/ml)	175.4 fg/ml (5959 proteins/ml)	$3.6x10^7$ copies/ml (Bojórquez-Velázquez et al. 2022) (~40,000 fg/ml)
Caffeine	10 fg/ml ($3.1x10^7$ molecules/ml)	2 fg/ml ($6.2x10^6$ molecules/ml)	5000 fg/ml (Huerta-Fontela, Galceran, and Ventura 2007)

361

medRxiv preprint doi: https://doi.org/10.1101/2024.03.18.24304492; this version posted March 19, 2024. The copyright holder for this preprint (which was not certified by peer review) is the author/funder, who has granted medRxiv a license to display the preprint in perpetuity. All rights reserved. No reuse allowed without permission.

In the case of LC-MS, LODs between 10^5 – 10^6 copies per nasopharynx sample (Dollman, Griffin, and Downard 2020; Nikolaev et al. 2020) have been reported. While LC-MS has been used to detect SARS-CoV-2 in wastewater (Peng et al. 2022; Lara-Jacobo et al. 2022), no detection limit has yet to be reported. So-called "rapid tests," on the other hand, while having short analysis time, typically rely on LFIA, which to the best of our knowledge have not shown the ability to rapidly sense the low level of virus in unprocessed wastewater. An LFIA sensed human adenovirus in processed wastewater by first concentrating the wastewater sample through PEG precipitation overnight and then performing a recombinase polymerase amplification step and achieving an LOD of 50 copies/reaction starting from an initial sample size of 1L (Rames and Macdonald 2019). While this is a low LOD, the tradeoff is in the time and complexity of the analysis.

3.2 Blind Testing

To ensure device integrity, a blind test in wastewater was performed. A single chip was functionalized with each virus aptamer in a different well. Four concentrations of each target protein were made by one author (O.R.P.) and were coded with a four-digit number (1738, 1993, 2930) with no indication of the contents. These were tested by another author (M.G.) using the same sensing protocol outlined above to determine which coded sample contained each protein. As shown in Fig. 6, for concentrations above 100 pg/mL (consistent with our earlier LOD) the target can easily be identified by only producing a Dirac shift in one well. Based on this, M.G. identified each target, which was confirmed

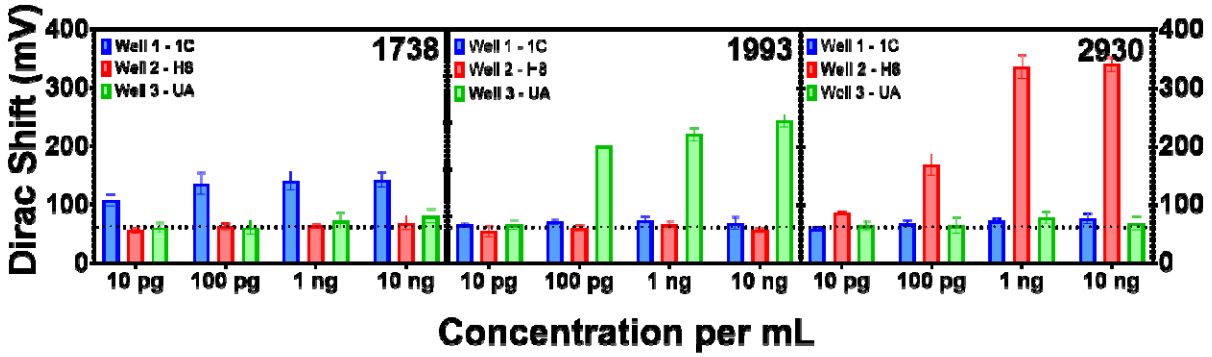

Fig. 6 – Wastewater Blind Tests: Each plot represents the differing concentrations for a coded sample. The assorted colors indicate the aptamer used in each well; blue for the 1C (Covid), red for H8 (RSV), and green for UA (Flu). The horizontal dotted line is the intrinsic shift from the wastewater. M.G. found that 1738 was COVID spike proteins (left), 1993 was HA (middle), and 2930 was RSV. Each was confirmed by O.R.P.'s written records.

medRxiv preprint doi: https://doi.org/10.1101/2024.03.18.24304492; this version posted March 19, 2024. The copyright holder for this preprint (which was not certified by peer review) is the author/funder, who has granted medRxiv a license to display the preprint in perpetuity. All rights reserved. No reuse allowed without permission.

correct by O.R.P.'s written records.

4. Conclusions and Future Work

To summarize, we showed the viability of our GEMS platform for selective, specific, simultaneous, and highly sensitive detection of four different analytes in wastewater, including caffeine for population normalization and three different viral proteins. We achieved limits of detection (see Table 1) one to two orders of magnitude better than HPLC-MS (Fig. 5) (Dollman, Griffin, and Downard 2020; Nikolaev et al. 2020; Peng et al. 2022; Lara-Jacobo et al. 2022; Kasprzyk-Hordern et al. 2023; Mestankova et al. 2012) and below the levels needed for effective early interventions (Peng et al. 2022). Results are obtained using a 1 cm^2 chip in just over one hour with minimal human intervention and without bulky, expensive lab equipment or costly reagents. Simple wastewater preparation can be easily performed with minimal training, while low voltage and resistance ranges can be operated with simple and cheap electronics. The cost is minimized by wafer-scale fabrication and pre-linked aptamers, further enhancing reproducibility and LOD. Combined with our previous results, the scalable GEMS platform enables rapid, easy, and cheap wastewater sensing of a wide range of analytes (opioid metabolites, viruses, etc.). This shows our platform to be a practical choice for wastewater-based epidemiology for viral testing and can lead to finding hotspots for future virus outbreaks. Our platform's low cost and power requirements could allow WBE to be performed on a building-by-building level in low-resource or rural settings, ushering in a new era of wastewater testing. Enabling this will require future efforts for on-chip electronics and microfluidics for sample preparation and a more comprehensive array of analytes to be tested on the same chip.

medRxiv preprint doi: https://doi.org/10.1101/2024.03.18.24304492; this version posted March 19, 2024. The copyright holder for this preprint (which was not certified by peer review) is the author/funder, who has granted medRxiv a license to display the preprint in perpetuity. All rights reserved. No reuse allowed without permission.

Author Information

Corresponding Author

Kenneth S. Burch – Department of Physics, Boston College, Chestnut Hill, Massachusetts 02467, United States; orcid.org/0000-0002-7541-0245; Email: ks.burch@bc.edu

Authors

Michael Geiwitz – Department of Physics, Boston College, Chestnut Hill, MA 02467, United States; orcid.org/0009-0000-7197-9381

Owen Rivers Page – Department of Biology, Boston College, Chestnut Hill, Massachusetts 02467, United States; orcid.org/0000-0003-4072-8509

Tio Marello – Department of Physics, Boston College, Chestnut Hill, MA 02467, United States

Narendra Kumar – GRIP Molecular Technologies, Inc., 1000 Westgate Drive, Saint Paul, MN 55114; orcid.org/0000-0002-5319-1547

Stephen Hummel – Department of Chemistry and Life Science, United States Military Academy, West Point, NY 10996, USA

Vsevolod Belosevich – Department of Physics, Boston College, Chestnut Hill, MA 02467, United States

Qiong Ma – Department of Physics, Boston College, Chestnut Hill, MA 02467, United States

Tim van Opijnen – Department of Biology, Boston College, Chestnut Hill, Massachusetts 02467, United States

Bruce Batten – GRIP Molecular Technologies, Inc., 1000 Westgate Drive, Saint Paul, MN 55114

Michelle M. Meyer – Department of Biology, Boston College, Chestnut Hill, Massachusetts 02467, United States; orcid.org/0000-0001-7014-9271

CRediT authorship contribution statement

K.S.B., M.G., and N.K. conceived the project and designed the experiments. M.G. fabricated, functionalized, and tested all GFET platforms. M.G., N.K., S.H, T.v.O., and K.S.B. selected all aptamers and analyzed the data. O.R.P. pre-linked all aptamers with PBASE linker molecules. T.M. aided in the design and placement of PDMS wells. S.H. validated 1C aptamer with flow cytometry. V.B. performed AFM and wire bonding machine maintenance. Q.M. supervised AFM and wire bonding maintenance.

medRxiv preprint doi: https://doi.org/10.1101/2024.03.18.24304492; this version posted March 19, 2024. The copyright holder for this preprint (which was not certified by peer review) is the author/funder, who has granted medRxiv a license to display the preprint in perpetuity. All rights reserved. No reuse allowed without permission.

T.v.O. supervised flow cytometry. M.M. supervised aptamer pre-linking and blind test sample preparation. B.B. and K.S.B. aided in data analysis. M.G., O.R.P., and K.S.B. wrote the manuscript.

Data Availability

All data is available on request.

Acknowledgements

The work of M.G., T.M., and K.S.B. are grateful for the support of the National Science Foundation (NSF) EPMD program via grant 2211334. M.M.M., K.S.B. and O.P are grateful for support from the Boston College Schiller Institute for Integrated Science and Society Exploratory Collaborative Scholarship grant. M.G. would like to thank the Boston College Cleanroom & Nanofabrication Facility's staff, Stephen Shepard and Dr. Chris Gunderson. M.G. and K.S.B. also thank Dr. Catherine Hoar for her insights on WBE. We would also like to thank Mr. Bryan Horsely, Mr. George Heufelder, and Dr. Sara Wigginton from MASSTC for providing wastewater samples and analysis of their source wastewater contents. Q.M. and V.B. acknowledge the American Chemical Society Petroleum Research Fund (PRF) 66299-DNI10.

References

Adams, Grace. 2020. "A Beginner's Guide to RT-PCR, QPCR and RT-QPCR." *The Biochemist* 42 (3): 48–53. https://doi.org/10.1042/BIO20200034.

Adelodun, Bashir, Fidelis Odedishemi Ajibade, Rahmat Gbemisola Ibrahim, Hashim Olalekan Bakare, and Kyung Sook Choi. 2020. "Snowballing Transmission of COVID-19 (SARS-CoV-2) through Wastewater: Any Sustainable Preventive Measures to Curtail the Scourge in Low-Income Countries?" *Science of the Total Environment* 742: 140680. https://doi.org/10.1016/j.scitotenv.2020.140680.

Ahmed, Warish, Nicola Angel, Janette Edson, Kyle Bibby, Aaron Bivins, Jake W. O'Brien, Phil M. Choi, et al. 2020. "First Confirmed Detection of SARS-CoV-2 in Untreated Wastewater in Australia: A Proof of Concept for the Wastewater Surveillance of COVID-19 in the Community." *Science of the Total Environment* 728: 138764. https://doi.org/10.1016/j.scitotenv.2020.138764.

Ahmed, Warish, Aaron Bivins, Mikayla Stephens, Suzanne Metcalfe, Wendy J M Smith, Kwanrawee Sirikanchana, Masaaki Kitajima, and Stuart L Simpson. 2023. "Occurrence of Multiple Respiratory Viruses in Wastewater in Queensland, Australia: Potential for Community Disease Surveillance." *Science of the Total Environment* 864: 161023. https://doi.org/10.1016/j.scitotenv.2022.161023.

medRxiv preprint doi: https://doi.org/10.1101/2024.03.18.24304492; this version posted March 19, 2024. The copyright holder for this preprint (which was not certified by peer review) is the author/funder, who has granted medRxiv a license to display the preprint in perpetuity. All rights reserved. No reuse allowed without permission.

Ahmed, Warish, Wendy J.M. Smith, Suzanne Metcalfe, Greg Jackson, Phil M. Choi, Mary Morrison, Daniel Field, et al. 2022. "Comparison of RT-QPCR and RT-DPCR Platforms for the Trace Detection of SARS-CoV-2 RNA in Wastewater." *ACS ES and T Water* 2 (11): 1871–80. https://doi.org/10.1021/ACSESTWATER.1C00387/ASSET/IMAGES/LARGE/EW1C00387_0001.JPEG.

Belter, Magdalena, Adam Sajnóg, and Danuta Barałkiewicz. 2014. "Over a Century of Detection and Quantification Capabilities in Analytical Chemistry-Historical Overview and Trends." https://doi.org/10.1016/j.talanta.2014.05.018.

Bhardwaj, Jyoti, Narendra Chaudhary, Hajin Kim, and Jaesung Jang. 2019. "Subtyping of Influenza A H1N1 Virus Using a Label-Free Electrochemical Biosensor Based on the DNA Aptamer Targeting the Stem Region of HA Protein." https://doi.org/10.1016/j.aca.2019.03.005.

Biobot. 2023a. "FAQ - Technical Questions: Results – Biobot Analytics." 2023. https://support.biobot.io/hc/en-us/articles/360052012934-FAQ-Technical-Questions-Results.

———. 2023b. "FAQ – Variant Sequencing – Biobot Analytics." 2023. https://support.biobot.io/hc/en-us/articles/14910772709527-FAQ-Variant-Sequencing.

Bojórquez-Velázquez, Esaú, Miriam Livier Llamas-García, José M. Elizalde-Contreras, Jesús Alejandro Zamora-Briseño, and Eliel Ruiz-May. 2022. "Mass Spectrometry Approaches for SARS-CoV-2 Detection: Harnessing for Application in Food and Environmental Samples." *Viruses 2022, Vol. 14, Page 872* 14 (5): 872. https://doi.org/10.3390/V14050872.

Cai, Shundong, Jianhua Yan, Hongjie Xiong, Yanfei Liu, Dongming Peng, and Zhenbao Liu. 2018. "Investigations on the Interface of Nucleic Acid Aptamers and Binding Targets." *Analyst* 143 (22): 5317–38. https://doi.org/10.1039/C8AN01467A.

Castro Neto, A H, F Guinea, N M R Peres, K S Novoselov, and A K Geim. 2009. "The Electronic Properties of Graphene." https://doi.org/10.1103/RevModPhys.81.109.

CDC. 2023. "Update on RSV and New Vaccine Recommendation | CDC." 2023. https://www.cdc.gov/respiratory-viruses/whats-new/rsv-update-2023-09-22.html.

Champredon, David, and Peter A. Vanrolleghem. 2023. "Editorial: Wastewater-Based Epidemiological Surveillance of Respiratory Pathogens." *Frontiers in Public Health* 11. https://doi.org/10.3389/FPUBH.2023.1328452.

Dollman, Nicholas L., Justin H. Griffin, and Kevin M. Downard. 2020. "Detection, Mapping, and Proteotyping of SARS-CoV-2 Coronavirus with High Resolution Mass Spectrometry." *ACS Infectious Diseases* 6 (12): 3269–76. https://doi.org/10.1021/ACSINFECDIS.0C00664.

Dong, Yongliang, Alex Lee, Deependra Kumar Ban, Kesong Wang, and Prabhakar Bandaru. 2023. "Femtomolar Level-Specific Detection of Lead Ions in Aqueous Environments, Using Aptamer-Derivatized Graphene Field-Effect Transistors." *ACS Applied Nano Materials* 6 (3): 2228–35. https://doi.org/10.1021/ACSANM.2C05542/ASSET/IMAGES/LARGE/AN2C05542_0005.JPEG.

Einav, Tal, Lauren E Gentles, and Jesse D Bloom. 2020. "SnapShot: Influenza by the Numbers." *Cell* 182. https://doi.org/10.1016/j.cell.2020.05.004.

Else, Laura, Victoria Watson, John Tjia, Andrew Hughes, Marco Siccardi, Saye Khoo, and David Back. 2010. "Validation of a Rapid and Sensitive High-Performance Liquid Chromatographyâ€"tandem Mass Spectrometry (HPLCâ€"MS/MS) Assay for the Simultaneous Determination of Existing and

medRxiv preprint doi: https://doi.org/10.1101/2024.03.18.24304492; this version posted March 19, 2024. The copyright holder for this preprint (which was not certified by peer review) is the author/funder, who has granted medRxiv a license to display the preprint in perpetuity. All rights reserved. No reuse allowed without permission.

New Antiretroviral Compounds." *Journal of Chromatography B* 878: 1455–65. https://doi.org/10.1016/j.jchromb.2010.03.036.

Fu, Wangyang, Cornelia Nef, Oren Knopfmacher, Alexey Tarasov, Markus Weiss, Michel Calame, and Christian Schönenberger. 2011. "Graphene Transistors Are Insensitive to PH Changes in Solution." *Nano Letters* 11 (9): 3597–3600. https://doi.org/10.1021/NL201332C/SUPPL_FILE/NL201332C_SI_001.PDF.

Fujii, Sho, Motohiro Kasuya, and Kazue Kurihara. 2017. "Characterization of Platinum Electrode Surfaces by Electrochemical Surface Forces Measurement." *Journal of Physical Chemistry C* 121 (47): 26406–13. https://doi.org/10.1021/ACS.JPCC.7B09301.

Gao, Ning, Teng Gao, Xiao Yang, Xiaochuan Dai, Wei Zhou, Anqi Zhang, and Charles M. Lieber. 2016. "Specific Detection of Biomolecules in Physiological Solutions Using Graphene Transistor Biosensors." *Proceedings of the National Academy of Sciences of the United States of America* 113 (51): 14633–38. https://doi.org/10.1073/PNAS.1625010114/-/DCSUPPLEMENTAL/PNAS.201625010SI.PDF.

Gosling, Jonathan H., Oleg Makarovsky, Feiran Wang, Nathan D. Cottam, Mark T. Greenaway, Amalia Patanè, Ricky D. Wildman, Christopher J. Tuck, Lyudmila Turyanska, and T. Mark Fromhold. 2021. "Universal Mobility Characteristics of Graphene Originating from Charge Scattering by Ionised Impurities." *Communications Physics* 4 (1). https://doi.org/10.1038/s42005-021-00518-2.

Goutelle, Sylvain, Michel Maurin, Florent Rougier, Xavier Barbaut, Laurent Bourguignon, Michel Ducher, and Pascal Maire. 2008. "The Hill Equation: A Review of Its Capabilities in Pharmacological Modelling." *Fundamental and Clinical Pharmacology*. https://doi.org/10.1111/j.1472-8206.2008.00633.x.

Gray, Mason J., Narendra Kumar, Ryan O'Connor, Marcel Hoek, Erin Sheridan, Meaghan C. Doyle, Marisa L. Romanelli, et al. 2020. "A Cleanroom in a Glovebox." *Review of Scientific Instruments* 91 (7): 073909. https://doi.org/10.1063/5.0006462.

Griffin, Justin H., and Kevin M. Downard. 2021. "Mass Spectrometry Analytical Responses to the SARS-CoV2 Coronavirus in Review." *TrAC Trends in Analytical Chemistry* 142 (September): 116328. https://doi.org/10.1016/J.TRAC.2021.116328.

Han, Mi Seon, Moon Woo Seong, Eun Young Heo, Ji Hong Park, Namhee Kim, Sue Shin, Sung Im Cho, Sung Sup Park, and Eun Hwa Choi. 2020. "Sequential Analysis of Viral Load in a Neonate and Her Mother Infected with Severe Acute Respiratory Syndrome Coronavirus 2." *Clinical Infectious Diseases* 71 (16): 2236–39. https://doi.org/10.1093/cid/ciaa447.

Hart, Olga E., and Rolf U. Halden. 2020. "Computational Analysis of SARS-CoV-2/COVID-19 Surveillance by Wastewater-Based Epidemiology Locally and Globally: Feasibility, Economy, Opportunities and Challenges." *Science of the Total Environment* 730: 138875. https://doi.org/10.1016/j.scitotenv.2020.138875.

Heijnen, Leo, and Gertjan Medema. 2011. "Surveillance of Influenza A and the Pandemic Influenza A (H1N1) 2009 in Sewage and Surface Water in the Netherlands." https://doi.org/10.2166/wh.2011.019.

Henze, Mogens; van Loosdrecht, Mark; Ekama, George; Brdjanovic, Damir. 2008. "Biological Wastewater Treatment - Google Books." In .

medRxiv preprint doi: https://doi.org/10.1101/2024.03.18.24304492; this version posted March 19, 2024. The copyright holder for this preprint (which was not certified by peer review) is the author/funder, who has granted medRxiv a license to display the preprint in perpetuity. All rights reserved. No reuse allowed without permission.

https://books.google.com/books?hl=en&lr=&id=41JButufnm8C&oi=fnd&pg=PA33&dq=wastewater+composition&ots=nUB5m3DG0n&sig=dZrAgPzlTTdRkngMOX-N3DoRvfM#v=onepage&q=wastewater composition&f=false.

Hsu, Shu Yu, Mohamed Bayati, Chenhui Li, Hsin Yeh Hsieh, Anthony Belenchia, Jessica Klutts, Sally A. Zemmer, et al. 2022. "Biomarkers Selection for Population Normalization in SARS-CoV-2 Wastewater-Based Epidemiology." *Water Research* 223 (September): 118985. https://doi.org/10.1016/J.WATRES.2022.118985.

https, Pearl, Vikram Srinivasa Raghavan, Theodore Bungon, Paul Davey, Toby Whitley, Shakil A Awan, and Sai Siva Gorthi. 2022. "Aptamer Functionalisation of Back-Gated Graphene Field Effect Transistors for Pb 2+ Sensing," 14–18. https://doi.org/10.3390/xxxxx.

Huang, Man Hong, Yong Mei Li, and Guo Wei Gu. 2010. "Chemical Composition of Organic Matters in Domestic Wastewater." *Desalination* 262 (1–3): 36–42. https://doi.org/10.1016/j.desal.2010.05.037.

Huang, Po Jung Jimmy, and Juewen Liu. 2022. "Selection of Aptamers for Sensing Caffeine and Discrimination of Its Three Single Demethylated Analogues." *Analytical Chemistry* 94 (7): 3142–49. https://doi.org/10.1021/ACS.ANALCHEM.1C04349/ASSET/IMAGES/LARGE/AC1C04349_0006.JPEG.

Huerta-Fontela, Maria, Maria Teresa Galceran, and Francesc Ventura. 2007. "Ultraperformance Liquid Chromatography Tandem Mass Spectrometry Analysis of Stimulatory Drugs of Abuse in Wastewater and Surface Waters." *Analytical Chemistry* 79 (10): 3821–29. https://doi.org/10.1021/AC062370X/ASSET/IMAGES/LARGE/AC062370XF00003.JPEG.

Hwang, Michael T., B. Landon Preston, Lee Joon, Choi Duyoung, H. Mo Alexander, Glinsky Gennadi, and Lal Ratnesh. 2016. "Highly Specific SNP Detection Using 2D Graphene Electronics and DNA Strand Displacement." *Proceedings of the National Academy of Sciences of the United States of America* 113 (26): 7088–93. https://doi.org/10.1073/PNAS.1603753113/SUPPL_FILE/PNAS.1603753113.SAPP.PDF.

Jones, David L., Marcos Quintela Baluja, David W. Graham, Alexander Corbishley, James E. McDonald, Shelagh K. Malham, Luke S. Hillary, et al. 2020. "Shedding of SARS-CoV-2 in Feces and Urine and Its Potential Role in Person-to-Person Transmission and the Environment-Based Spread of COVID-19." *The Science of the Total Environment* 749 (December): 141364. https://doi.org/10.1016/J.SCITOTENV.2020.141364.

Jones, Susan, David T.A. Daley, Nicholas M. Luscombe, Helen M. Berman, and Janet M. Thornton. 2001. "Protein–RNA Interactions: a Structural Analysis." *Nucleic Acids Research* 29 (4): 943. https://doi.org/10.1093/NAR/29.4.943.

Karthikeyan, Smruthi, Joshua I Levy, Peter De Hoff, Greg Humphrey, Amanda Birmingham, Kristen Jepsen, Sawyer Farmer, et al. 2022. "Wastewater Sequencing Reveals Early Cryptic SARS-CoV-2 Variant Transmission." *Nature* 609 (7925): 101–8. https://doi.org/10.1038/s41586-022-05049-6.

Karthikeyan, Smruthi, Andrew Nguyen, Daniel McDonald, Yijian Zong, Nancy Ronquillo, Junting Ren, Jingjing Zou, et al. 2021. "Rapid, Large-Scale Wastewater Surveillance and Automated COVID-19 Cases on a University Campus." *American Society for Microbiology* 6 (4): e00793-21.

Kasprzyk-Hordern, Barbara, Natalie Sims, Kata Farkas, Kishore Jagadeesan, Kathryn Proctor, Matthew J. Wade, and Davey L. Jones. 2023. "Wastewater-Based Epidemiology for Comprehensive Community

medRxiv preprint doi: https://doi.org/10.1101/2024.03.18.24304492; this version posted March 19, 2024. The copyright holder for this preprint (which was not certified by peer review) is the author/funder, who has granted medRxiv a license to display the preprint in perpetuity. All rights reserved. No reuse allowed without permission.

Health Diagnostics in a National Surveillance Study: Mining Biochemical Markers in Wastewater." *Journal of Hazardous Materials* 450 (January): 130989. https://doi.org/10.1016/j.jhazmat.2023.130989.

Ke, Zunlong, Joaquin Oton, Kun Qu, Mirko Cortese, Vojtech Zila, Lesley McKeane, Takanori Nakane, et al. 2020. "Structures and Distributions of SARS-CoV-2 Spike Proteins on Intact Virions." *Nature 2020 588:7838* 588 (7838): 498–502. https://doi.org/10.1038/s41586-020-2665-2.

Khan, Niazul I., and Edward Song. 2021. "Detection of an IL-6 Biomarker Using a GFET Platform Developed with a Facile Organic Solvent-Free Aptamer Immobilization Approach." *Sensors 2021, Vol. 21, Page 1335* 21 (4): 1335. https://doi.org/10.3390/S21041335.

Kohlberger, Michael, and Gabriele Gadermaier. 2022. "SELEX: Critical Factors and Optimization Strategies for Successful Aptamer Selection." *Biotechnology and Applied Biochemistry* 69 (5): 1771. https://doi.org/10.1002/BAB.2244.

Kumar, Narendra, Mason Gray, Juan C. Ortiz-Marquez, Andrew Weber, Cameron R Desmond, Avni Argun, Tim Opijnen, and Kenneth S Burch. 2020. "Detection of a Multi-disease Biomarker in Saliva with Graphene Field Effect Transistors." *MEDICAL DEVICES & SENSORS*, October, e10121. https://doi.org/10.1002/mds3.10121.

Kumar, Narendra, Muhit Rana, Michael Geiwitz, Niazul Islam Khan, Matthew Catalano, Juan C Ortiz-Marquez, Hikari Kitadai, et al. 2022. "Rapid, Multianalyte Detection of Opioid Metabolites in Wastewater." *ACS Nano* 16 (3): 3704–14. https://doi.org/10.1021/acsnano.1c07094.

Kumar, Narendra, Wenjian Wang, Juan C. Ortiz-Marquez, Matthew Catalano, Mason Gray, Nadia Biglari, Kitadai Hikari, et al. 2020. "Dielectrophoresis Assisted Rapid, Selective and Single Cell Detection of Antibiotic Resistant Bacteria with G-FETs." *Biosensors and Bioelectronics* 156 (February): 112123. https://doi.org/10.1016/j.bios.2020.112123.

Kwong Hong Tsang, Deana, Tyler J. Lieberthal, Clare Watts, Iain E. Dunlop, Sami Ramadan, Armando E. del Rio Hernandez, and Norbert Klein. 2019. "Chemically Functionalised Graphene FET Biosensor for the Label-Free Sensing of Exosomes." *Scientific Reports 2019 9:1* 9 (1): 1–10. https://doi.org/10.1038/s41598-019-50412-9.

Lafond, Kathryn E., Rachael M. Porter, Melissa J. Whaley, Zhou Suizan, Zhang Ran, Mohammad Abdul Aleem, Binay Thapa, et al. 2021. "Global Burden of Influenza-Associated Lower Respiratory Tract Infections and Hospitalizations among Adults: A Systematic Review and Meta-Analysis." *PLOS Medicine* 18 (3): e1003550. https://doi.org/10.1371/JOURNAL.PMED.1003550.

Lara-Jacobo, Linda R., Golam Islam, Jean Paul Desaulniers, Andrea E. Kirkwood, and Denina B.D. Simmons. 2022. "Detection of SARS-CoV-2 Proteins in Wastewater Samples by Mass Spectrometry." *Environmental Science and Technology* 56 (8): 5062–70. https://doi.org/10.1021/ACS.EST.1C04705/ASSET/IMAGES/LARGE/ES1C04705_0005.JPEG.

Leung, Nancy H L. 2021. "Transmissibility and Transmission of Respiratory Viruses." https://doi.org/10.1038/s41579-021-00535-6.

Li, Wnkui; Zhang, Ji; Tse, Francis L.S. 2013. *Handbook of LC-MS Bioanalysis: Best Practices, Experimental Protocols, and ... - Google Books*. https://books.google.com/books?hl=en&lr=&id=xz7AEAAAQBAJ&oi=fnd&pg=PR11&dq=lc-ms+protocol&ots=jwlHekwcxh&sig=gS2EDkTDLMpJFwfYtcF65uTIv2A#v=onepage&q=lc-ms

medRxiv preprint doi: https://doi.org/10.1101/2024.03.18.24304492; this version posted March 19, 2024. The copyright holder for this preprint (which was not certified by peer review) is the author/funder, who has granted medRxiv a license to display the preprint in perpetuity. All rights reserved. No reuse allowed without permission.

protocol&f=false.

Li, Chenhui, Mohamed Bayati, Shu-Yu Hsu, Hsin-Yeh Hsieh, Wilfing Lindsi, Anthony Belenchia, Sally A. Zemmer, et al. 2022a. "Population Normalization in SARS-CoV-2 Wastewater-Based Epidemiology: Implications from Statewide Wastewater Monitoring in Missouri." *MedRxiv*, September, 2022.09.08.22279459. https://doi.org/10.1101/2022.09.08.22279459.

———. 2022b. "Population Normalization in SARS-CoV-2 Wastewater-Based Epidemiology: Implications from Statewide Wastewater Monitoring in Missouri." *MedRxiv*, September, 2022.09.08.22279459. https://doi.org/10.1101/2022.09.08.22279459.

Li, Jiahao, Ding Wu, Yi Yu, Tingxian Li, Kun Li, Meng Meng Xiao, Yirong Li, Zhi Yong Zhang, and Guo Jun Zhang. 2021. "Rapid and Unamplified Identification of COVID-19 with Morpholino-Modified Graphene Field-Effect Transistor Nanosensor." *Biosensors and Bioelectronics* 183 (July): 113206. https://doi.org/10.1016/J.BIOS.2021.113206.

Lorenzo, Maria, and Yolanda Picó. 2019. "Wastewater-Based Epidemiology: Current Status and Future Prospects." *Current Opinion in Environmental Science and Health* 9: 77–84. https://doi.org/10.1016/j.coesh.2019.05.007.

Lores, Emile M., and Jonathan R. Pennock. 1998. "The Effect of Salinity on Binding of Cd, Cr, Cu and Zn to Dissolved Organic Matter." *Chemosphere* 37 (5): 861–74. https://doi.org/10.1016/S0045-6535(98)00090-3.

Lowry, Sarah A., Marlene K. Wolfe, and Alexandria B. Boehm. 2023. "Respiratory Virus Concentrations in Human Excretions That Contribute to Wastewater: A Systematic Review and Meta-Analysis." *Journal of Water and Health* 21 (6): 831–48. https://doi.org/10.2166/WH.2023.057.

Lu, Hsiang Wei, Alexander A. Kane, Jonathan Parkinson, Yingning Gao, Reza Hajian, Michael Heltzen, Brett Goldsmith, and Kiana Aran. 2022. "The Promise of Graphene-Based Transistors for Democratizing Multiomics Studies." *Biosensors and Bioelectronics* 195 (January): 113605. https://doi.org/10.1016/J.BIOS.2021.113605.

Madhi, Shabir A., Fernando P. Polack, Pedro A. Piedra, Flor M. Munoz, Adrian A. Trenholme, Eric A.F. Simões, Geeta K. Swamy, et al. 2020. "Respiratory Syncytial Virus Vaccination during Pregnancy and Effects in Infants." *New England Journal of Medicine* 383 (5): 426–39. https://doi.org/10.1056/NEJMOA1908380/SUPPL_FILE/NEJMOA1908380_DATA-SHARING.PDF.

Massano, Marta, Alberto Salomone, Enrico Gerace, Eugenio Alladio, Marco Vincenti, and Marco Minella. 2023. "Wastewater Surveillance of 105 Pharmaceutical Drugs and Metabolites by Means of Ultra-High-Performance Liquid-Chromatography-Tandem High Resolution Mass Spectrometry." *Journal of Chromatography. A* 1693: 463896. https://doi.org/10.1016/j.chroma.2023.463896.

Medema, Gertjan, Frederic Been, Leo Heijnen, and Susan Petterson. 2020. "Implementation of Environmental Surveillance for SARS-CoV-2 Virus to Support Public Health Decisions: Opportunities and Challenges." *Current Opinion in Environmental Science and Health* 17: 49–71. https://doi.org/10.1016/j.coesh.2020.09.006.

Mestankova, Hana, Kristin Schirmer, Beate I. Escher, Urs Von Gunten, and Silvio Canonica. 2012. "Removal of the Antiviral Agent Oseltamivir and Its Biological Activity by Oxidative Processes." *Environmental Pollution* 161: 30–35. https://doi.org/10.1016/j.envpol.2011.09.018.

Metabolite, Molnupiravir, Timofey Komarov, Polina Karnakova, Olga Archakova, Dana Shchelgacheva,

medRxiv preprint doi: https://doi.org/10.1101/2024.03.18.24304492; this version posted March 19, 2024. The copyright holder for this preprint (which was not certified by peer review) is the author/funder, who has granted medRxiv a license to display the preprint in perpetuity. All rights reserved. No reuse allowed without permission.

Natalia Bagaeva, Mariia Popova, et al. 2023. "Chromatography with Tandem Mass Spectrometry (HPLC-MS/MS) Method for Quantification of Major Development and Validation of a High-Performance Liquid Chromatography with Tandem Mass Spectrometry (HPLC-MS/MS) Method for Quantification of Major Molnupiravir Metabolite (β-D-N4-Hydroxycytidine) in Human Plasma." https://doi.org/10.3390/biomedicines11092356.

Nekrasov, Nikita, Stefan Jaric, Dmitry Kireev, Aleksei V. Emelianov, Alexey V. Orlov, Ivana Gadjanski, Petr I. Nikitin, Deji Akinwande, and Ivan Bobrinetskiy. 2022. "Real-Time Detection of Ochratoxin A in Wine through Insight of Aptamer Conformation in Conjunction with Graphene Field-Effect Transistor." *Biosensors and Bioelectronics* 200 (March): 113890. https://doi.org/10.1016/J.BIOS.2021.113890.

Nemudryi, Artem, Anna Nemudraia, Tanner Wiegand, Kevin Surya, Murat Buyukyoruk, Calvin Cicha, Karl K. Vanderwood, Royce Wilkinson, and Blake Wiedenheft. 2020. "Temporal Detection and Phylogenetic Assessment of SARS-CoV-2 in Municipal Wastewater." *Cell Reports Medicine* 1 (6). https://doi.org/10.1016/J.XCRM.2020.100098.

Nikolaev, Evgeny N., Maria I. Indeykina, Alexander G. Brzhozovskiy, Anna E. Bugrova, Alexey S. Kononikhin, Natalia L. Starodubtseva, Evgeny V. Petrotchenko, Grigoriy I. Kovalev, Christoph H. Borchers, and Gennady T. Sukhikh. 2020. "Mass-Spectrometric Detection of SARS-CoV-2 Virus in Scrapings of the Epithelium of the Nasopharynx of Infected Patients via Nucleocapsid N Protein." *Journal of Proteome Research* 19 (11): 4393–97. https://doi.org/10.1021/ACS.JPROTEOME.0C00412/ASSET/IMAGES/MEDIUM/PR0C00412_0003.GIF.

Novo, Ana, Sandra André, Paula Viana, Olga C. Nunes, and Célia M. Manaia. 2013. "Antibiotic Resistance, Antimicrobial Residues and Bacterial Community Composition in Urban Wastewater." *Water Research* 47 (5): 1875–87. https://doi.org/10.1016/j.watres.2013.01.010.

Pan, Yang, Daitao Zhang, Peng Yang, Leo L.M. Poon, and Quanyi Wang. 2020. "Viral Load of SARS-CoV-2 in Clinical Samples." *The Lancet. Infectious Diseases* 20 (4): 411. https://doi.org/10.1016/S1473-3099(20)30113-4.

Pawar, Pratik. 2023. "Tracking RSV in Low- and Middle-Income Countries." *Nature* 621 (7980): S62–63. https://doi.org/10.1038/D41586-023-02960-4.

Peccia, Jordan, Alessandro Zulli, Doug E. Brackney, Nathan D. Grubaugh, Edward H. Kaplan, Arnau Casanovas-Massana, Albert I. Ko, et al. 2020. "Measurement of SARS-CoV-2 RNA in Wastewater Tracks Community Infection Dynamics." *Nature Biotechnology* 38 (10): 1164. https://doi.org/10.1038/S41587-020-0684-Z.

Peng, Jiaxi, Jianxian Sun, Minqing Ivy Yang, Richard M. Gibson, Eric J. Arts, Abayomi S. Olabode, Art F.Y. Poon, et al. 2022. "Early Warning Measurement of SARS-CoV-2 Variants of Concern in Wastewaters by Mass Spectrometry." *Environmental Science and Technology Letters* 9 (7): 638–44. https://doi.org/10.1021/ACS.ESTLETT.2C00280/ASSET/IMAGES/LARGE/EZ2C00280_0003.JPEG.

Percze, Krisztina, Zoltán Szakács, Éva Scholz, Judit András, Zsuzsanna Szeitner, Corné H Van Den Kieboom, Gerben Ferwerda, Marien I De Jonge, Róbert E Gyurcsányi, and Tamás Mészáros. 2017. "Aptamers for Respiratory Syncytial Virus Detection OPEN." https://doi.org/10.1038/srep42794.

Picó, Yolanda, and Damià Barceló. 2021. "Mass Spectrometry in Wastewater-Based Epidemiology for the Determination of Small and Large Molecules as Biomarkers of Exposure: Toward a Global View of

medRxiv preprint doi: https://doi.org/10.1101/2024.03.18.24304492; this version posted March 19, 2024. The copyright holder for this preprint (which was not certified by peer review) is the author/funder, who has granted medRxiv a license to display the preprint in perpetuity. All rights reserved. No reuse allowed without permission.

Environment and Human Health under the COVID-19 Outbreak." *ACS Omega* 6 (46): 30865–72. https://doi.org/10.1021/ACSOMEGA.1C04362/ASSET/IMAGES/LARGE/AO1C04362_0002.JPEG.

Ping, Jinglei, Ramya Vishnubhotla, Amey Vrudhula, and A. T.Charlie Johnson. 2016a. "Scalable Production of High-Sensitivity, Label-Free DNA Biosensors Based on Back-Gated Graphene Field Effect Transistors." *ACS Nano* 10 (9): 8700–8704. https://doi.org/10.1021/ACSNANO.6B04110/ASSET/IMAGES/LARGE/NN-2016-04110P_0005.JPEG.

Ping, Jinglei, Ramya Vishnubhotla, Amey Vrudhula, and A T Charlie Johnson. 2016b. "Scalable Production of High-Sensitivity, Label-Free DNA Biosensors Based on Back-Gated Graphene Field Effect Transistors." *Acs Nano* 10 (9): 8700–8704. https://doi.org/10.1021/acsnano.6b04110.

Pinto, Artur M., Inês C. Gonçalves, and Fernão D. Magalhães. 2013. "Graphene-Based Materials Biocompatibility: A Review." *Colloids and Surfaces B: Biointerfaces* 111 (November): 188–202. https://doi.org/10.1016/J.COLSURFB.2013.05.022.

Qian, Shuwen, Dingran Chang, Sisi He, and Yingfu Li. 2022. "Aptamers from Random Sequence Space: Accomplishments, Gaps and Future Considerations." *Analytica Chimica Acta* 1196 (March): 339511. https://doi.org/10.1016/J.ACA.2022.339511.

Rainey, Andrew L., Song Liang, Joseph H. Bisesi, Tara Sabo-Attwood, and Anthony T. Maurelli. 2023. "A Multistate Assessment of Population Normalization Factors for Wastewater-Based Epidemiology of COVID-19." *PLOS ONE* 18 (4): e0284370. https://doi.org/10.1371/JOURNAL.PONE.0284370.

Rames, Emily K., and Joanne Macdonald. 2019. "Rapid Assessment of Viral Water Quality Using a Novel Recombinase Polymerase Amplification Test for Human Adenovirus." *Applied Microbiology and Biotechnology* 103 (19): 8115–25. https://doi.org/10.1007/S00253-019-10077-W/TABLES/2.

Rodrigues, Teresa, Vladyslav Mishyn, Yann R. Leroux, Laura Butruille, Eloise Woitrain, Alexandre Barras, Patrik Aspermair, et al. 2022. "Highly Performing Graphene-Based Field Effect Transistor for the Differentiation between Mild-Moderate-Severe Myocardial Injury." *Nano Today* 43: 101391. https://doi.org/10.1016/j.nantod.2022.101391.

Rouzé, Anahita, Ignacio Martin-Loeches, Pedro Povoa, Demosthenes Makris, Antonio Artigas, Mathilde Bouchereau, Fabien Lambiotte, et al. 2021. "Relationship between SARS-CoV-2 Infection and the Incidence of Ventilator-Associated Lower Respiratory Tract Infections: A European Multicenter Cohort Study." *Intensive Care Med* 47: 188–98. https://doi.org/10.1007/s00134-020-06323-9.

Sender, Ron, Yinon M. Bar-On, Shmuel Gleizer, Biana Bernsthein, Avi Flamholz, Rob Phillips, and Ron Milo. 2020. "The Total Number and Mass of SARS-CoV-2 Virions." *MedRxiv*, November. https://doi.org/10.1101/2020.11.16.20232009.

Seo, Giwan, Geonhee Lee, Mi Jeong Kim, Seung Hwa Baek, Minsuk Choi, Keun Bon Ku, Chang Seop Lee, et al. 2020a. "Rapid Detection of COVID-19 Causative Virus (SARS-CoV-2) in Human Nasopharyngeal Swab Specimens Using Field-Effect Transistor-Based Biosensor." *ACS Nano* 14 (4): 5135–42. https://doi.org/10.1021/ACSNANO.0C02823/ASSET/IMAGES/LARGE/NN0C02823_0006.JPEG.

———. 2020b. "Rapid Detection of COVID-19 Causative Virus (SARS-CoV-2) in Human Nasopharyngeal Swab Specimens Using Field-Effect Transistor-Based Biosensor." *ACS Nano* 14 (4): 5135–42. https://doi.org/10.1021/ACSNANO.0C02823/ASSET/IMAGES/LARGE/NN0C02823_0006.JPEG.

Shiratori, Ikuo, Joe Akitomi, David A. Boltz, Katsunori Horii, Makio Furuichi, and Iwao Waga. 2014.

medRxiv preprint doi: https://doi.org/10.1101/2024.03.18.24304492; this version posted March 19, 2024. The copyright holder for this preprint (which was not certified by peer review) is the author/funder, who has granted medRxiv a license to display the preprint in perpetuity. All rights reserved. No reuse allowed without permission.

"Selection of DNA Aptamers That Bind to Influenza A Viruses with High Affinity and Broad Subtype Specificity." *Biochemical and Biophysical Research Communications* 443 (1): 37–41. https://doi.org/10.1016/j.bbrc.2013.11.041.

Stern, Eric. 2007. "Label-Free Sensing with Semiconducting Nanowires."

Street, Renée, Shirley Malema, Nomfundo Mahlangeni, and Angela Mathee. 2020. "Wastewater Surveillance for Covid-19: An African Perspective." *Science of the Total Environment* 743: 2018–20. https://doi.org/10.1016/j.scitotenv.2020.140719.

Sweetapple, Chris, Matthew J. Wade, Peter Melville-Shreeve, Albert S. Chen, Chris Lilley, Jessica Irving, Jasmine M.S. Grimsley, and Joshua T. Bunce. 2023. "Dynamic Population Normalisation in Wastewater-Based Epidemiology for Improved Understanding of the SARS-CoV-2 Prevalence: A Multi-Site Study." *Journal of Water and Health* 21 (5): 625–42. https://doi.org/10.2166/WH.2023.318.

Szunerits, Sabine, Teresa Rodrigues, Rupali Bagale, Henri Happy, Rabah Boukherroub, and Wolfgang Knoll. 2023. "Graphene-Based Field-Effect Transistors for Biosensing: Where Is the Field Heading To?" *Analytical and Bioanalytical Chemistry*, June, 1–14. https://doi.org/10.1007/S00216-023-04760-1/TABLES/1.

Urmann, Katharina, Julia Modrejewski, Thomas Scheper, and Johanna G. Walter. 2017. "Aptamer-Modified Nanomaterials: Principles and Applications." *BioNanoMaterials* 18 (1–2): 20160012. https://doi.org/10.1515/BNM-2016-0012/ASSET/GRAPHIC/J_BNM-2016-0012_FIG_001.JPG.

Velusamy, Karthik, Selvakumar Periyasamy, P Senthil Kumar, Gayathri Rangasamy, J Mercy, Nisha Pauline, Pradeep Ramaraju, Sneka Mohanasundaram, and Dai-Viet Nguyen Vo. 2022. "Biosensor for Heavy Metal Detection in Wastewater: A Review." *Food and Chemical Toxicology* 168: 278–6915. https://doi.org/10.1016/j.fct.2022.113307.

Wang, Chih-Hung, Chih-Peng Chang, and Gwo-Bin Lee. 2016. "Integrated Microfluidic Device Using a Single Universal Aptamer to Detect Multiple Types of Influenza Viruses $." https://doi.org/10.1016/j.bios.2016.06.071.

Wang, Hao, Zhuang Hao, Cong Huang, Feiran Li, and Yunlu Pan. 2023. "Monitoring Cd 2+ in Oily Wastewater Using an Aptamer-Graphene Field-Effect Transistor with a Selective Wetting Surface †." https://doi.org/10.1039/d2na00416j.

Wölfel, Roman, Victor M. Corman, Wolfgang Guggemos, Michael Seilmaier, Sabine Zange, Marcel A. Müller, Daniela Niemeyer, et al. 2020. "Virological Assessment of Hospitalized Patients with COVID-2019." *Nature 2020 581:7809* 581 (7809): 465–69. https://doi.org/10.1038/s41586-020-2196-x.

World Health Organization. 2014. "The Top 10 Causes of Death." 2014. https://www.who.int/news-room/fact-sheets/detail/the-top-10-causes-of-death.

Wu, Guangfu, Xin Tang, M Meyyappan, and King Wai Chiu Lai. 2017. "Doping Effects of Surface Functionalization on Graphene with Aromatic Molecule and Organic Solvents." *Applied Surface Science* 425: 713–21. https://doi.org/10.1016/j.apsusc.2017.07.048.

Wu, Yuangen, Shenshan Zhan, Lumei Wang, and Pei Zhou. 2014. "Selection of a DNA Aptamer for Cadmium Detection Based on Cationic Polymer Mediated Aggregation of Gold Nanoparticles." *Analyst* 139 (6): 1550–61. https://doi.org/10.1039/C3AN02117C.

medRxiv preprint doi: https://doi.org/10.1101/2024.03.18.24304492; this version posted March 19, 2024. The copyright holder for this preprint (which was not certified by peer review) is the author/funder, who has granted medRxiv a license to display the preprint in perpetuity. All rights reserved. No reuse allowed without permission.

783 Zang, Ruochen, Maria Florencia Gomez Castro, Broc T. McCune, Qiru Zeng, Paul W. Rothlauf, Naomi M.
784 Sonnek, Zhuoming Liu, et al. 2020. "TMPRSS2 and TMPRSS4 Promote SARS-CoV-2 Infection of
785 Human Small Intestinal Enterocytes." *Science Immunology* 5 (47).
786 https://doi.org/10.1126/SCIIMMUNOL.ABC3582.

787 Zhang, Ning, Yuhuan Gong, Fanping Meng, Yuhai Bi, Penghui Yang, and Fusheng Wang. 2020. "Virus
788 Shedding Patterns in Nasopharyngeal and Fecal Specimens of COVID-19 Patients." *MedRxiv*, March,
789 2020.03.28.20043059. https://doi.org/10.1101/2020.03.28.20043059.

790 Zhang, Yang, Mario Juhas, and Chun Kit Kwok. 2022. "Aptamers Targeting SARS-COV-2: A Promising Tool
791 to Fight against COVID-19." https://doi.org/10.1016/j.tibtech.2022.07.012.

792 Zhang, Zijie, Richa Pandey, Jiuxing Li, Jimmy Gu, Dawn White, Hannah D. Stacey, Jann C. Ang, et al. 2021.
793 "High-Affinity Dimeric Aptamers Enable the Rapid Electrochemical Detection of Wild-Type and
794 B.1.1.7 SARS-CoV-2 in Unprocessed Saliva." *Angewandte Chemie - International Edition* 60 (45):
795 24266–74. https://doi.org/10.1002/ANIE.202110819.

796 Zhou, Jiehua, and John Rossi. 2017. "Aptamers as Targeted Therapeutics: Current Potential and
797 Challenges." *Nature Reviews. Drug Discovery* 16 (3): 181. https://doi.org/10.1038/NRD.2016.199.

798

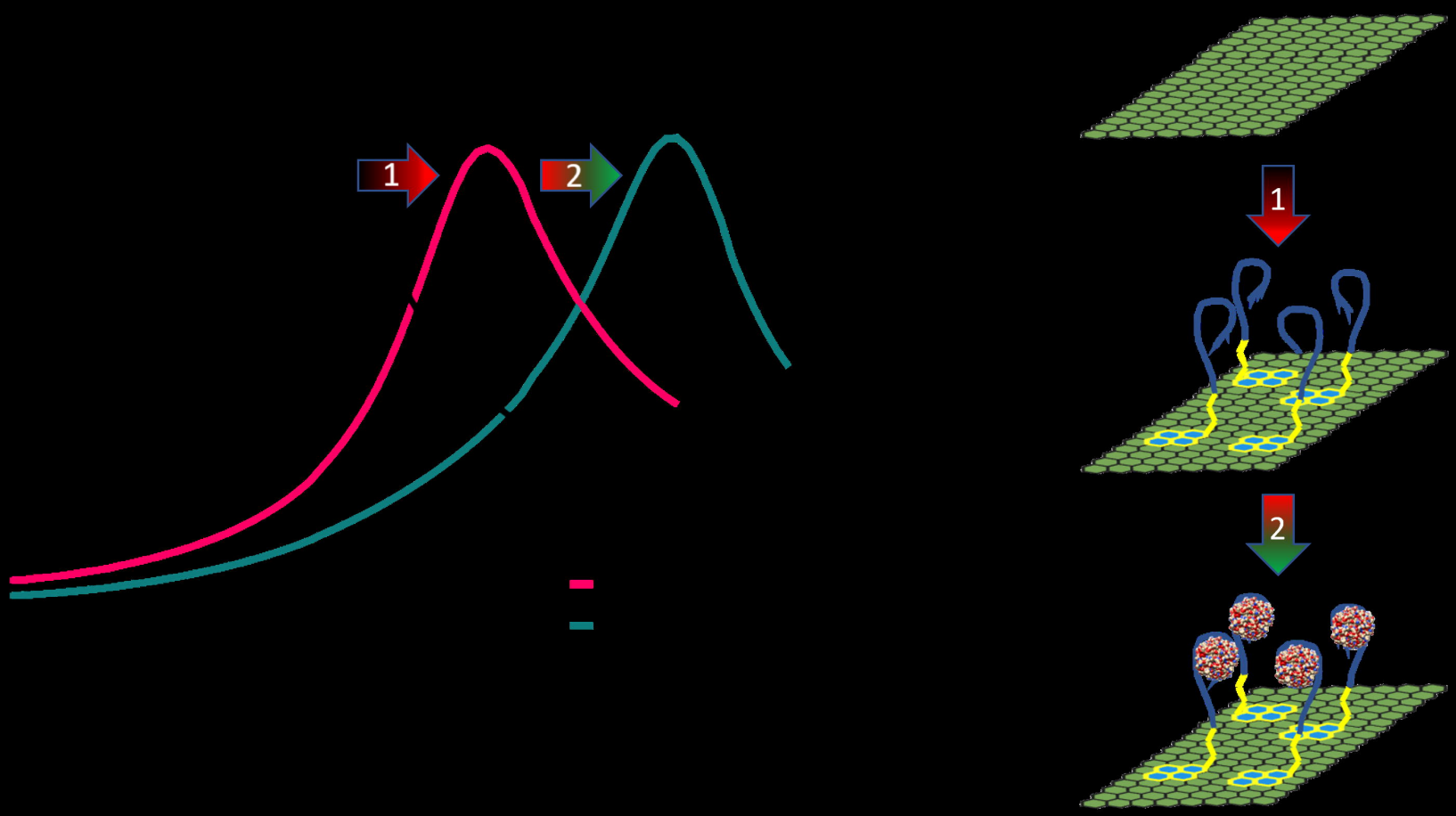

Fig. 1 – Dirac voltage shifting with aptamer and target attachment: The plot on the left shows the positive shift in the Dirac point (peak of the curves) from the intrinsic position of the bare graphene (black) of approximately 0.6V. After a 2:1 mixture of the aptamer probe to PEG is added the Dirac point shifts positively to about 0.8V (pink). A large shift in the Dirac point to 1.2V is then seen (green) in the presence of 1ng/ml of the target protein for SARS-CoV-2. On the right is a schematic of the bare graphene, aptamer attachment, and target attachment.

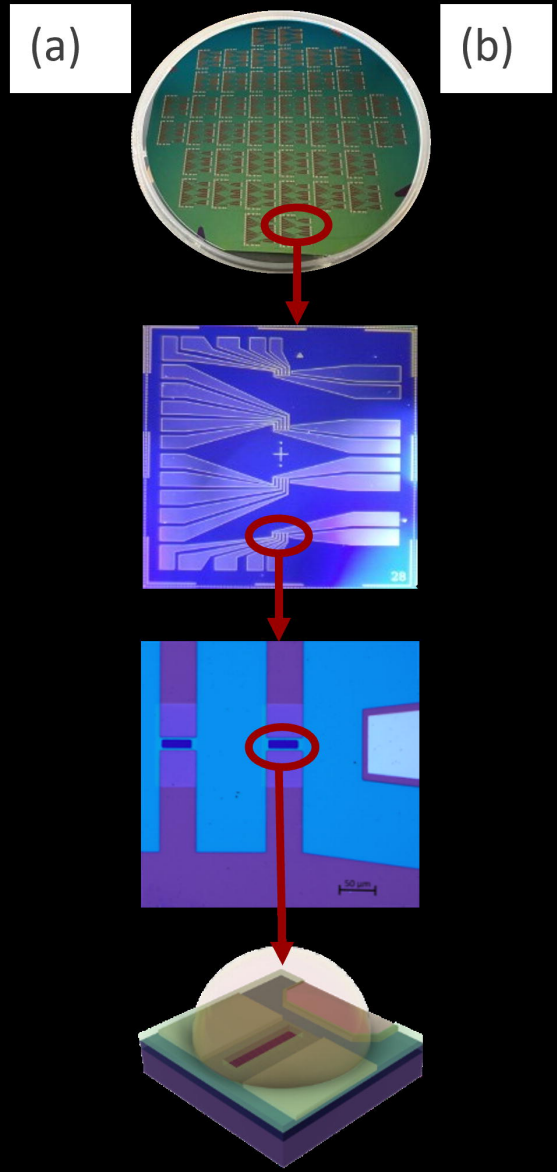

Fig. 2 – (a) Top: Wafer as fully fabricated. Second from top: Overview of the 1.2cm x 1.2cm GFET sensing platform. Third from top: 20x microscope image of a single sensing well. Two graphene devices and the coplanar gate electrode are shown. Bottom: Diagram of a single, functionalized graphene device during the sensing process. (b) Schematic of individual chip with PDMS well and labeled with functionalization for specific analytes.

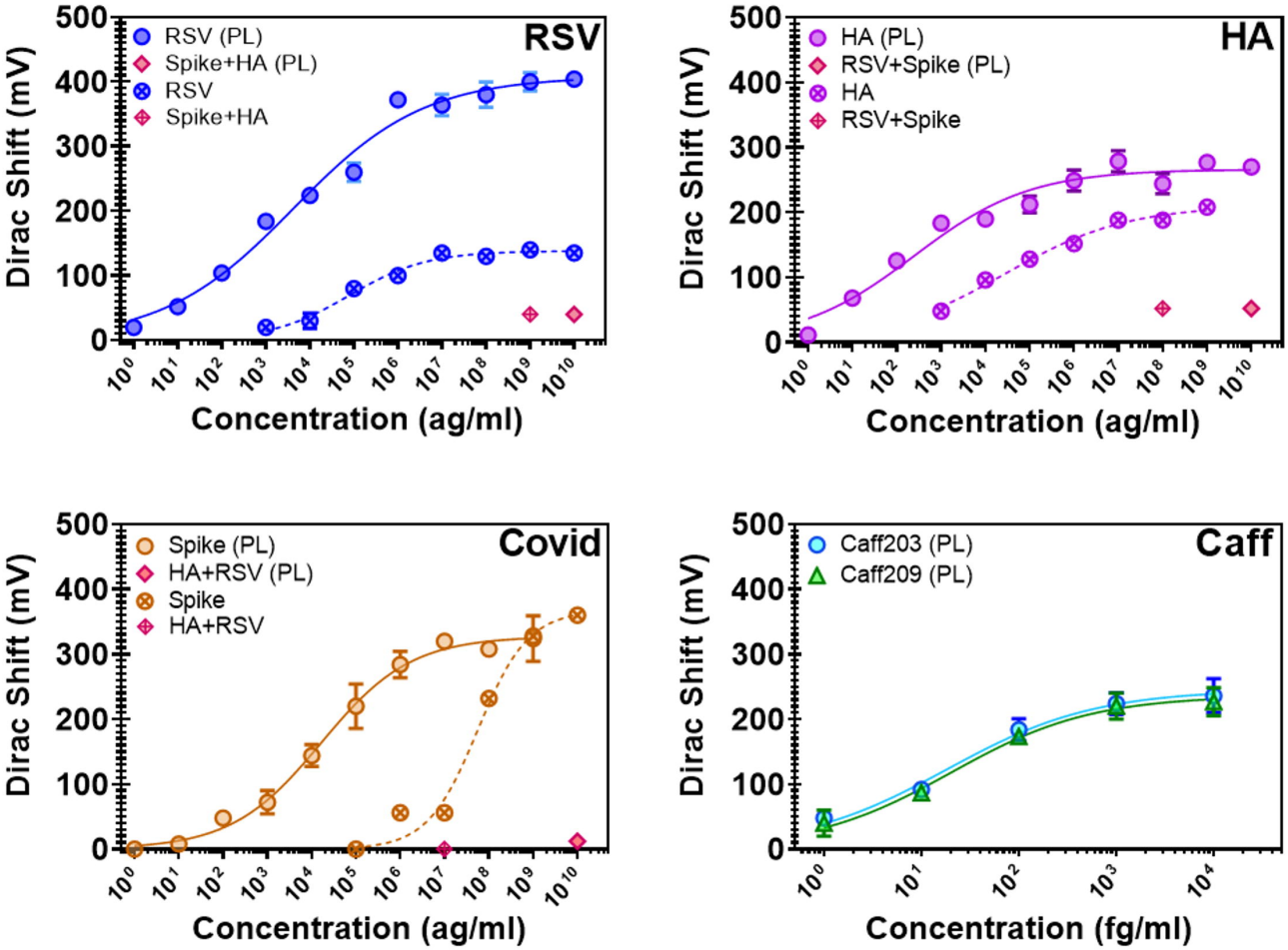

Fig. 3 –Concentration dependance measurements of viral proteins in PBS. Error bars calculated from the five GFETs per sensing well. Data points with crosses and dashed curves indicate non-pre-linked aptamers were used. Top Left - Influenza A Hemagglutinin detection. High concentrations of RSV and COVID Spike proteins used as a negative control. (PL) denotes pre-linked aptamer experiment. Top Right and Bottom Left - Same as in HA plot but with SARS-CoV-2 Spike and RSV proteins, respectively. Non-target proteins used as negative control in each case. Bottom Right - Concentration dependence measurements of two caffeine aptamers. Caffeine measurements were only conducted with pre-linked aptamers.

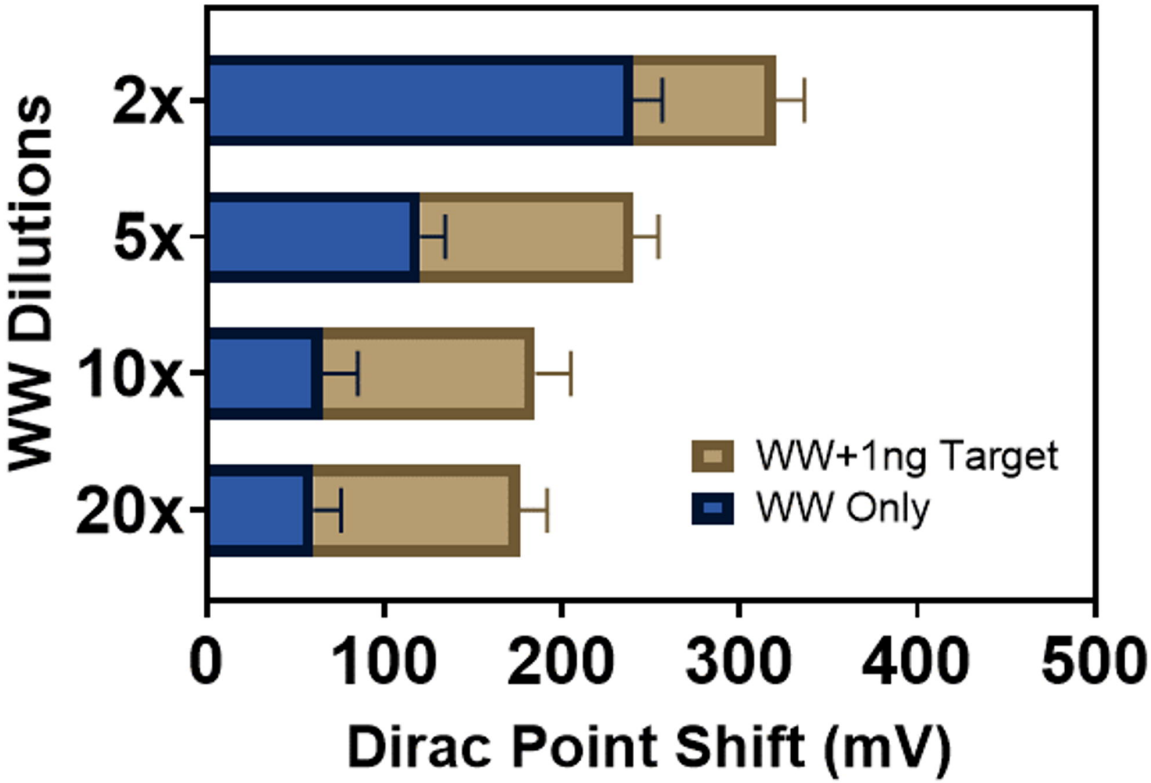

Fig. 4 – Histogram of the average Dirac point shift at various wastewater dilutions. The blue areas show the average Dirac point shift for five GFET devices after incubation of diluted wastewater for one hour. The tan areas show the further Dirac point shift after incubating the GFETs for one hour with 1ng/ml of target protein in their respective wastewater dilutions.

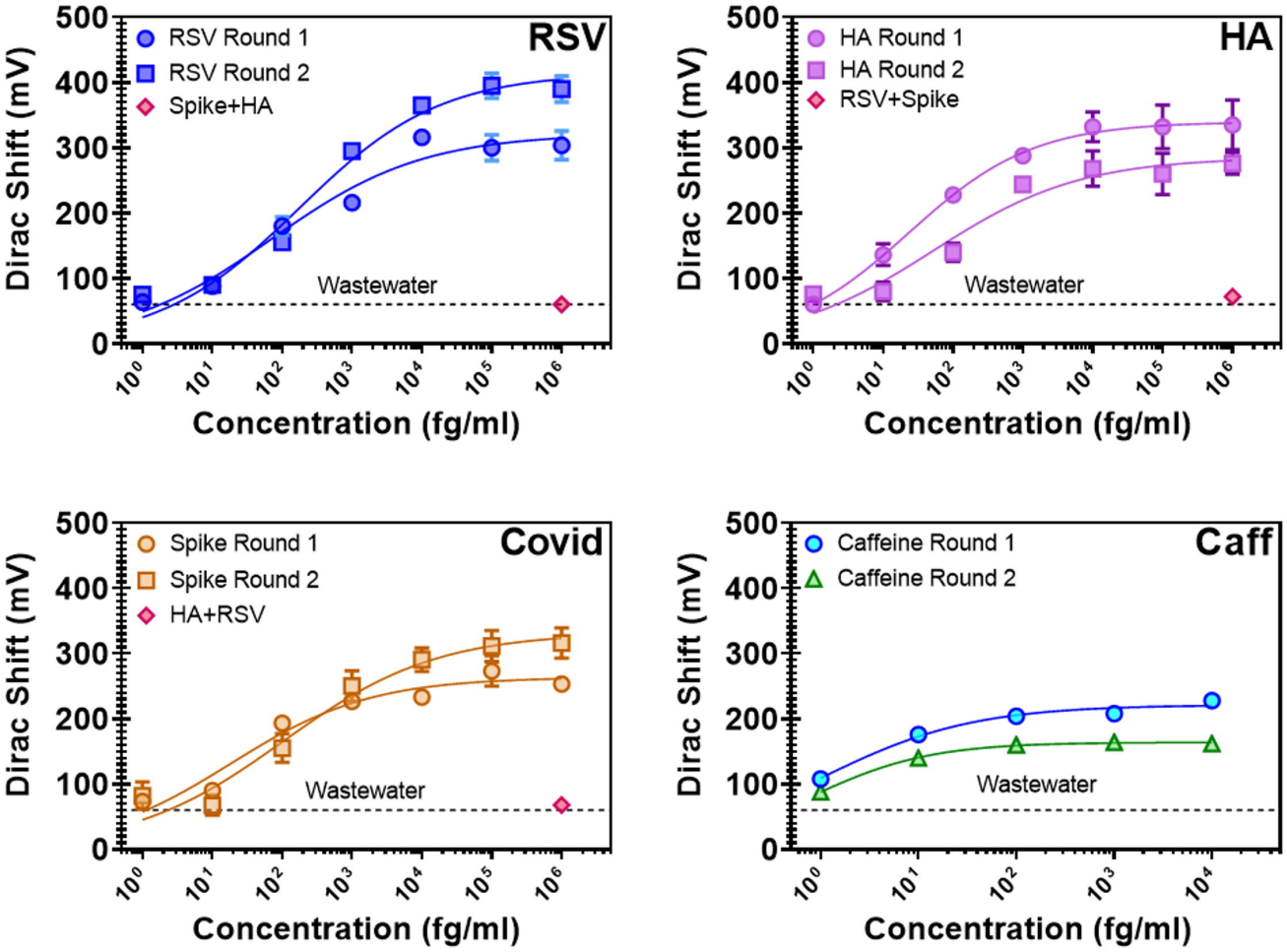

Fig. 5 – Concentration dependence measurements of viral proteins and caffeine in wastewater. Error bars calculated from the five GFETs per sensing well. From left to right, HA, RSV, and COVID spike proteins and Caffeine. Horizontal dashed line shows intrinsic background shift from the wastewater itself.

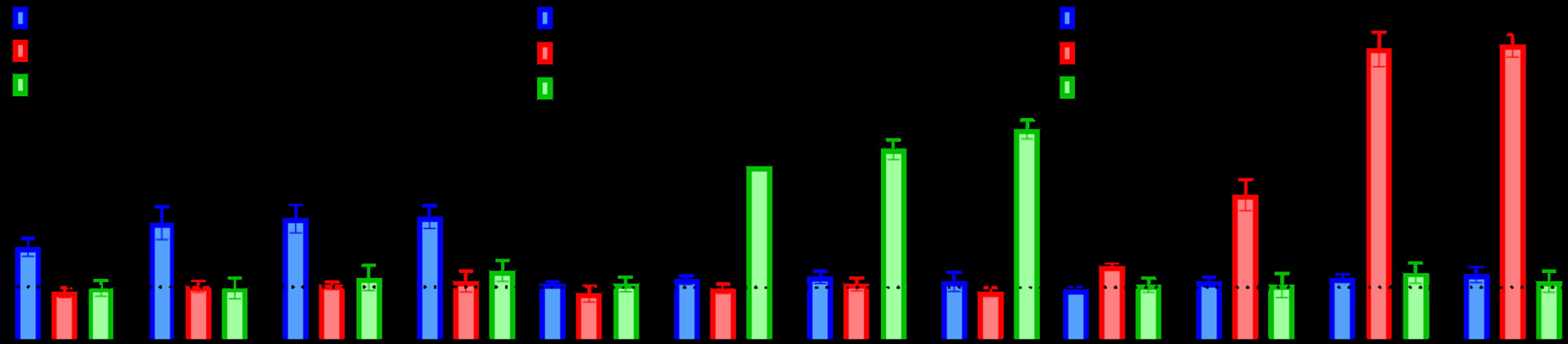

Fig. 6 – Wastewater Blind Tests: Each plot represents the differing concentrations for a coded sample. The assorted colors indicate the aptamer used in each well; blue for the 1C (Covid), red for H8 (RSV), and green for UA (Flu). The horizontal dotted line is the intrinsic shift from the wastewater. M.G. found that 1738 was COVID spike proteins (left), 1993 was HA (middle), and 2930 was RSV. Each was confirmed by O.R.P.'s written records.